

**ÇUKUROVA UNIVERSITY
INSTITUTE OF NATURAL AND APPLIED SCIENCES**

MSc THESIS

Yunus Emre TÜRKOĞLU

**ECONOMIC ANALYSIS OF ABSORPTION COOLING SYSTEM WITH
NATURAL GAS IN ÇUKUROVA REGION**

DEPARTMENT OF MECHANICAL ENGINEERING

ADANA,2009

ÇUKUROVA ÜNİVERSİTESİ
FEN BİLİMLERİ ENSTİTÜSÜ

**ECONOMIC ANALYSIS OF ABSORPTION COOLING SISTEM WITH
NATURAL GAS IN ÇUKUROVA REGION**

Yunus Emre TÜRKOĞLU

YÜKSEK LİSANS TEZİ

MAKİNA MÜHENDİSLİĞİ ANABİLİM DALI

**Bu tez 06/07/2009 Tarihinde Aşağıdaki Jüri Üyeleri Tarafından
Oybirliği/Oyçokluğu ile Kabul Edilmiştir.**

İmza: İmza: İmza:
Yrd.Doç.Dr. Alper YILMAZ Doç.Dr. Hüseyin AKILLI Yrd.Doç.Dr. Nihat ÇELİK
DANIŞMAN ÜYE ÜYE

Bu Tez Enstitümüz Makine Mühendisliği Anabilim Dalında Hazırlanmıştır.

Kod No:

Prof.Dr. Aziz ERTUNÇ
Enstitü Müdürü

Not: Bu tezde kullanılan özgün ve başka kaynaktan yapılan bildirişlerin, çizelge, şekil ve fotoğrafların kaynak gösterilmeden kullanımı, 5846 sayılı Fikir ve Sanat Eserleri Kanunundaki hükümlere tabidir.

ABSTRACT

MSc THESIS

<p>ECONOMIC ANALYSIS OF ABSORPTION COOLING SISTEM WITH NATURAL GAS IN ÇUKUROVA REGION</p>
--

Yunus Emre TÜRKOĞLU

**DEPARTMENT OF MECHANICAL ENGINEERING
INSTITUTE OF NATURAL AND APPLIED SCIENCES
UNIVERSITY OF ÇUKUROVA**

Supervisor : Assist. Prof. Dr. Alper YILMAZ
Year : 2009, Pages:75
Jury : Assist. Prof. Dr. Alper YILMAZ
Assoc. Prof. Dr. Hüseyin AKILLI
Assist. Prof. Dr. Nihat ÇELİK

In this study, cooling systems using natural gas with cost analysis are studied. In addition, conventional vapor compression refrigeration systems and absorption cooling systems activated with natural gas are compared. The cooling of a place with a cooling load of 200.000 kcal/h with absorption cooling system activated with natural gas is studied. The coefficient of performance (COP) of the system dependent on evaporator, absorber, condenser and generator temperatures was predicted with Artificial Neural Network (ANN) model. As a result, energy costs of absorption cooling systems activated with natural gas are appeared more economic cooling systems than conventional vapor compression systems.

Keywords: Air-conditioning, absorption cooling, economical analysis

ÖZ

YÜKSEK LİSANS TEZİ

ÇUKUROVA BÖLGESİNDE DOĞALGAZLI ABSORPSİYONLU SOĞUTMA SİSTEMİNİN EKONOMİK ANALİZİ

Yunus Emre TÜRKOĞLU

ÇUKUROVA ÜNİVERSİTESİ
FEN BİLİMLERİ ENSTİTÜSÜ
MAKİNA MÜHENDİSLİĞİ ANABİLİM DALI

Danışman : Yrd. Doç. Dr. Alper YILMAZ
Yıl : 2009, Sayfa: 75
Jüri : Yrd. Doç. Dr. Alper YILMAZ
Doç. Dr. Hüseyin AKILLI
Yrd. Doç. Dr. Nihat ÇELİK

Bu çalışmada; doğalgaz ve absorpsiyonlu soğutma sistemleri incelenerek, doğal gazla çalışan absorpsiyonlu soğutma sistemlerinin maliyet analizi yapılmıştır. Ayrıca buhar sıkıştırımlı mekanik sistemler ile doğalgazlı absorpsiyonlu soğutma sistemleri karşılaştırılmıştır. 200.000 kcal/h'lik soğutma ihtiyacı olan bir mekanın, doğalgazlı absorpsiyonlu soğutma sistemiyle boyutlandırılması yapılmıştır. Sistemin etkinliği (COP), buharlaştırıcı, soğurucu, yoğuşturucu ve ayırıcı sıcaklıklarına bağlı olarak Yapay Sinir Ağları (YSA) modeliyle tahmin edilmiştir. Bu tezde sonuç olarak absorpsiyonlu ve buhar sıkıştırımlı soğutma sistemlerinin ekonomik karşılaştırması yapılmış, doğalgazlı absorpsiyonlu soğutma sistemlerinin enerji maliyeti olarak daha ekonomik soğutma sistemleri olduğu ortaya çıkmıştır.

Anahtar Kelimeler: İklimlendirme, absorpsiyonlu soğutma, ekonomik analiz

ACKNOWLEDGEMENTS

Thanks are extended to my research adviser Assist. Prof. Dr. Alper YILMAZ, for his advice, invaluable guidance, understanding and support throughout the preparation of this thesis and during my graduate education.

I am truly grateful to Prof. Dr. Orhan BÜYÜKALACA, for providing valuable research advice, continuous support and understanding during my thesis.

I also thank to my committee member, Assos. Prof. Dr. Hüseyin AKILLI and Assist. Prof. Dr. Nihat ÇELİK for his support and many helpful suggestions.

I want to express my sincere appreciation to research assistants of the Mechanical Engineering Department of Çukurova University for their help, support and motivation.

In additional, I would like to especially thank to my wife and family.

CONTENTS	PAGE
ABSTRACT.....	I
ÖZ.....	II
ACKNOWLEDGEMENTS.....	III
TABLE OF CONTENTS.....	IV
LIST OF TABLES.....	VI
LIST OF FIGURES.....	VII
NOMENCLATURE.....	IX
1. INTRODUCTION.....	1
2. LITERATURE REVIEW.....	3
3. MATERIAL AND METHOD.....	9
3.1. Absorption Cooling Systems.....	9
3.2. Working Principle of Absorption Cooling Systems.....	11
3.3. Types of Absorption Cooling Systems.....	13
3.3.1. Single Effect Absorption Cooling Systems.....	14
3.3.2. Double effect Absorption Cooling Systems.....	15
3.3.3. Triple effect Absorption Cooling Systems.....	16
3.3.4. Hybrid Absorption Cooling Systems.....	16
3.4. Advantages of Absorption Cooling Systems.....	17
3.5. Absorption Cooling Applications.....	18
3.6. Absorption Cooling Systems with Natural Gas.....	18
3.7. Description of Absorption Cooling System Studied.....	19
3.8. Cooling Load Profile of Air Conditioning Place.....	25
3.9. Description of Artificial Neural Network (ANN) model..	25
3.10. Modeling of the thermodynamic properties with ANN....	26
3.11. Description of Vapor Compression Cooling Systems.....	34
3.12. Vapor Compression Cooling Cycle Analysis.....	36
3.13. Thermodynamic Modeling of Vapor Compression Cooling System.....	38
3.14. Natural Gas Consumption of Absorption Cooling System	42

3.15. Electricity Consumption of Vapor Compression Cooling System.....	44
3.16. Economic Analysis of a Project.....	46
3.16.1. Identification and Quantification of Benefits..	46
3.16.2. Identification and Quantification of Costs.....	46
3.16.3. System Costs.....	47
3.16.4. Time Value of Money.....	47
3.16.5. Simple Payback Period Method.....	48
3.16.6. Net Present Value Method.....	49
3.16.7. Internal Rate of Return Method.....	50
4. RESULTS AND DISCUSSION.....	52
5. CONCLUSIONS.....	64
REFERANCES.....	66
CURRICULUM VITAE.....	69
APPENDIX.....	70

LIST OF TABLES	PAGE
Table 3.1. Energy-mass balance equations of absorption system components.....	27
Table 3.2. Parameters and temperature intervals of absorption system.....	28
Table 3.3. Statistical results of thermodynamic properties with ANN.....	30
Table 3.4. COP values of absorption cooling systems compared with the real and calculated with ANN	33
Table 3.5. Hourly natural gas consumption of absorption cooling system	43
Table 3.6. Monthly electricity consumption of vapor compression cooling system.....	45
Table 3.7. Various situations of NPV.....	50
Table 4.1. The values and results used in absorption cooling system calculated with ANN.....	54
Table 4.2. Monthly operation costs of absorption cooling system in 2006.....	60
Table 4.3. Monthly operation costs of vapor compression cooling system in 2006.....	61
Table 4.4. Costs and parameters for economical analysis.....	62
Table 4.5. Economical analysis of absorption and vapor compression cooling systems.....	63

LIST OF FIGURES	PAGE
Figure 3.1. Components of the absorption cooler compared with a compression cooler.....	9
Figure 3.2. Arrangement of the components of absorption.....	12
Figure 3.3. Comparison of COPs for multistage absorption chillers	13
Figure 3.4. Single-effect absorption refrigeration cycle.....	14
Figure 3.5. Double-effect absorption -refrigeration cycle.....	15
Figure 3.6. Triple-effect absorption cycle.....	16
Figure 3.7. Electricity and natural gas consumption presentation....	20
Figure 3.8. A double effect direct fired absorption chiller schematic diagram.....	21
Figure 3.9. A double effect direct fired absorption cycle.....	22
Figure 3.10. Information for processing artificial neural network unit	26
Figure 3.11. Schematic representation of the absorption cooling system	27
Figure 3.12. ANN model used for COP prediction.....	29
Figure 3.13. Layout of the vapor compression refrigeration system...	34
Figure 3.14. Temperature- Entropy diagram for vapor compression System.....	35
Figure 3.15. Pressure-Enthalpy diagram of refrigerant R410A.....	39
Figure 3.16. Distribution COP-electricity consumption year of 2006..	45
Figure 4.1. Distribution of COP and temperature of absorption cooling system in the year 2006.....	53
Figure 4.2. Distribution of COP and temperature of absorption cooling system in July-2006.....	55
Figure 4.3. Distribution of COP and temperature of absorption cooling system in 21 March 2006.....	56
Figure 4.4. Distribution of COP and NGC monthly year of 2006.....	57
Figure 4.5. Distribution of COP and NGC daily year of 2006.....	58

Figure 4.6.	Distribution of COP and temperature vapor compression cooling system.....	59
Figure 4.7.	Distribution of COP and EC monthly for the year 2006	59
Figure 4.8.	Comparison of operation costs for absorption and vapor compression cooling systems.....	61

NOMENCLATURE

ANN	Artificial neural network
TRNSYS	The transient energy system simulation tool
CFC	Chlorofluorocarbon
COP	Coefficient of performance
HVAC	Heating, ventilating and air conditioning
Q_E	Heat load in the evaporator (kcal/h)
Q_G	Heat load in the generator (kcal/h)
\dot{m}	Mass flow rate (kg/s)
h	Enthalpy (kJ/kg)
Q_A	Heat load in the absorber (kcal/h)
Q_C	Heat load in the condenser (kcal/h)
T_{Gh}	High temperature generator ($^{\circ}\text{C}$)
T_{Gl}	Low temperature generator ($^{\circ}\text{C}$)
T_E	Evaporator temperature ($^{\circ}\text{C}$)
T_C	Condenser temperature ($^{\circ}\text{C}$)
T_A	Absorber temperature ($^{\circ}\text{C}$)
η	Efficiency
RMS	Root mean squared
cov	Permutation coefficient
R^2	Absolute permutation percentage
P	Pressure (N/m^2)
ν	Specific volume (m^3/kg)
s	entropy (kJ/kgK)
ε	Dead volume ratio
M_R	Refrigerant flow rate (kg/s)
V_R	Volumetric flow rate of the refrigerant (m^3/s)
η_m	Mechanical efficiency

NGC	natural gas consumption (m^3/h)
Q_G	Heat load in the generator (kcal/h)
η	Burning efficiency of the natural gas
LTV	Low heating value for natural gas (kcal/m^3)
EC	Electricity consumption (kW/h)
Q_C	Heat load in the compressor (kcal/h)
η	Efficiency of the electricity
LTV	Lower heating value for electricity generation (kcal/kW)
FV	Future value of the investment
PV	Present Value of the investment
i	Interest rate (%)
NPV	Net Present Value
IRR	Internal rate of return
DCFROR	Discounted cash flow rate of return
ROR	Rate of return
F_n	Benefit in year n

1.INTRODUCTION

From the beginning of the 19th century, absorption cooling systems attracted increasing interest, since it is possible to recover energy by using waste heat and thermal solar energy with these systems for cooling applications. Absorption coolers have been mass-produced since the 1960s. Absorption chillers differ from the more prevalent compression chillers in the way that the cooling effect is driven by heat energy rather than mechanical energy. When the absorption chillers are examined from constructional points of view, the components of them should be integrated much more closely than the components of a vapor compression cooling system. In all large absorption systems, cooling is distributed by chilled water. Similarly, all condensers are cooled by water, usually from a cooling tower (Wulfinghoff 2003).

The most commonly used pairs of working fluids are ammonia-water and water- LiBr. For ammonia-water systems, ammonia is the refrigerant and the water is solvent, while for water-LiBr systems water is the refrigerant and LiBr is the solvent. Temperature ranges of the machines are determined by the thermodynamic properties of the refrigerant. The boiling temperature of the ammonia at 105 kPa is 33°C, which enables the machines with ammonia-water pairs to be used for freezing. However, refrigerant water is only available at temperatures above 0°C, which makes it possible to use for cooling and air-conditioning (Herold et al. 1996, Srihirin et al. 2001). In LiBr systems, the extremely low refrigerant pressure, which is around 103 kPa at 5°C is favorable for low values of pump power and uncomplicated constructions. Another advantage of the LiBr systems is the high boiling point distance between the refrigerant and the solvent, which creates a pure refrigerant vapor when the refrigerant is expelled from the solution. In ammonia-water systems, the boiling point distance is only around 133 K, which results in boiling of some water (solvent). This solvent should be removed from the refrigerant vapor in a rectifying column. The main drawback of the LiBr systems is the possibility of the solvent to be crystallized. If during the expulsion of the refrigerant, the refrigerant concentration in the solution drops too sharply, it can cause the remained solvent to be crystallized. This leads to a malfunction of the machine (Eicker 2003).

Natural gas cooling systems have greater resource efficiency than similar electric systems. Typical electricity generation and distribution result in an approximately 65% - 75% loss in the initial energy resource of the fuel. In contrast, only about 5% to 10% of the fuel resource is lost with a gas system.

Gas absorption systems have several non-energy benefits over conventional electric systems including:

- ◆ Elimination of the use of CFC and HCFC refrigerants
- ◆ Quiet, vibration-free operation
- ◆ Lower pressure systems with no large rotating components
- ◆ High reliability
- ◆ Low maintenance

The contribution that gas cooling technologies can make to the goal of improved emissions is substantial. Natural gas-powered air-conditioning equipment offers substantial advantages to the environment in regard to CFCs and HCFCs, because they are not used in the absorption cycle. Legislative activities are focused on pushing the nation toward energy-efficient technologies that reduce harmful emissions. While gas-fired chillers produce emissions at the site, combustion efficiencies can be high and harmful emissions comparatively low for a well-operated absorption unit.

In this study; the cooling of a place which required 200.000 kcal/h cooling load using absorption cooling system activated with natural gas is studied and compared to conventional cooling systems.

2.LITERATURE REVIEW

Romera et al. (1998) modeled a thermodynamic analysis carried out to compare the theoretical performance of single stage, two stage and double-absorption heat transformers operating with the water/lithium bromide and the water/Carrol mixtures, where Carrol is a mixture of lithium bromide and ethylene glycol $[(\text{CH}_2\text{OH})_2]$ (in the ratio 1:4) by weight. A mathematical model to predict the theoretical performance of single stage and the advanced heat transformers is also described. Coefficients of performance and gross temperature lifts are compared for the different heat transformers and plotted against the main temperatures of the system for both mixtures. The water/Carrol mixture showed in general to have a better performance than the water/lithium bromide mixture.

Castells et al. (2000) proposed to the economic optimization of an energy plant that interacts with a refrigeration cycle, by using a successive linear programming technique (SLP). The aim of this paper is to study the viability of the integration of already technologically available absorption chillers in CHP plants. The results of this alternative are compared with the results obtained using the conventional way of producing chilled water, that is, using mechanical vapor compression chillers in order to select the best refrigeration cycle alternative for a given refrigeration demand. This approach is implemented in the computer program and tested using the data obtained in the water/LiBr absorption chiller of Bayer in Tarragona (Catalonia, Spain). The results clearly show that absorption chiller is a good option not only when low-cost process heat is available, but also when a cogeneration system is present. The absorption chiller acts as a bottoming cycle by using steam generated in the heat recovery boiler. In this way, the cogeneration size can be increased producing higher benefits than those obtained with the use of compression chillers.

Renganarayanan et al. (2005) presented and discussed steady state modeling of a double effect absorption chiller using steam as heat input. The modeling is based on the artificial neural network (ANN) technique with 6-6-9-1 configuration. The neural network is a fully connected feed forward configuration using the back

propagation learning algorithm. The model will predict the chiller performance based on the chilled water inlet and outlet temperatures, cooling water inlet and outlet temperatures and steam pressure. The network was trained with one year of experimental data and predicts the performance within $\pm 1.2\%$ of the actual values.

Park et al. (2006) performed a lumped-parameter dynamic simulation of a single-effect ammonia-water absorption chiller. Modeling is based on the continuity of species constituting the ammonia-water mixture and the conservation of energy for each component of the absorption chiller. Ordinary differential equations governing the response of each component and the algebraic equations describing the constitutive relation are solved in parallel by numerical integration. The model has been applied to a commercially available 10.5 kW absorption chiller to study the transients of temperature, pressure, concentration, and void fraction of each component during the start-up operation. The time constant of the absorption chiller is also investigated. The parameters considered are the bulk concentration of the ammonia-water solution, the mass of the solution filled, and the volumes of key components of the absorption chiller. In addition, the reduction of the time constant by a stepwise turn-up and turndown of the flue gas flow rate during the primary stage of start-up period is demonstrated.

Pinazo et al. (2002) the performance data related to direct-fired double-effect water–lithium bromide absorption chillers in air conditioning systems are scarce. The knowledge of these data is important to validate the models that predict their performance, as well as to establish the design criteria and control strategies that lead to an optimal performance of these machines in air conditioning systems. The objectives of this work were to acquire and analyze the performance data of a 105 kW direct-fired double-effect water–lithium bromide absorption chiller, to simulate with TRNSYS the performance of an air conditioning system in which this machine operates, and to compare the recorded data with the results obtained from simulation. The use of a steady-state model for the absorption machine predicted energy consumption 30% lower than that registered at the air conditioning system. This difference was due to the effect of the transient performance of the absorption chiller, not considered by the employed model.

Gupta et al. (2001) studied the application of thermo-economic theory to the economic optimization of a single effect water/LiBr vapor absorption refrigeration system for air-conditioning application which aimed at minimizing its overall operation and amortization costs. They explained the mathematical models and showed that numerical techniques based optimization of thermal system is not always possible due to plant complexities. Therefore, a simplified cost minimization methodology is applied to evaluate the economic costs of all the internal flows and products of the system by formulating economic cost equations. Once these costs are determined, the system is thermo-economically evaluated to identify the effects of design variables on costs and enables to suggest values of design variables that would make the overall system cost effective. They showed that approximate optimum design configuration is obtained by means of sequential local optimization of the system, carried out unit by unit. The result compares this optimum with the base case and shows percentage variations in the system's operation and amortization costs.

Givois et al. (1994) presented the dynamic modeling of an absorption system and an application to a large air-conditioned system. This study was performed using the ALLAN. Simulation software has a pre and post processor enabling the symbolic description of systems. The absorption system is a direct gas double effect absorption chiller or heater, using LiBr/HB₂BO as working fluid. Their modeling has two aims. The first one is to optimize the water circuit by determining the volume of a storage tank that maximize the energetically and economic operation performances. The second objective is to evaluate by simulation the influence of the previous results on a large air-conditioned system and over given periods. They describe the modeling approach and the results are compared with measurements monitored during summer 1994. The models created are available for use by engineers for sizing, optimizing or doing economic evaluation of HVAC systems.

Şencan et al. (2005) analyzed the thermodynamic analysis of the sorption refrigeration systems. They presented a new approach to performance analysis of double-effect sorption refrigeration systems. Fluid couple LiBr + LiNO₃ + LiI + LiCl / H₂O (mole ratio LiBr:LiNO:LiI:LiCl = 5:1:1:2, respectively) which do not cause

ozone depletion in the system was used. The Coefficient of Performance (COP) of system dependent on evaporator, absorber, condenser and generator temperatures was predicted with Artificial Neural Network (ANN) model. The back-propagation learning algorithm with two different variants and logistic sigmoid transfer function were used in the ANN. In order to train the neural network, limited literature data were used. In order to determine COP of system, a new formulation was derived by very well trained ANN model ($R^2= 0,9939$) in the study.

Yakut et al. (2004) studied thermodynamic analysis of absorption systems. The limited experimental data and analytical functions required for calculating the thermodynamic properties of fluid pairs, which usually involves the solution of complex differential equations. In order to simplify this complex process, Artificial Neural Networks (ANNs) are used. They presented a new approach for the determination of the thermodynamic properties of LiBr–water and LiCl–water solutions which have been the most widely used in the absorption heat pump systems. Instead of complex differential equations and limited experimental data, faster and simpler solutions were obtained by using equations derived from the ANN model. It was found that the coefficient of multiple determination (R^2 -value) between the actual and ANN predicted data is equal to about 0.999 for the enthalpy of both LiBr–water and LiCl–water solutions. As seen from the results obtained, the calculated thermodynamic properties are obviously within acceptable limits. In addition, the coefficient of performance (COP) of absorption systems operating under different conditions with LiBr–water and LiCl–water solutions is calculated.

Lecuona et al. (2002) studied low-temperature heat (between 5°C and 90°C) to drive absorption systems in two different applications: refrigeration and heat pump cycles. Double and triple stage absorption systems are modeled and simulated, allowing a comparison between the absorbent–refrigerant solutions H_2O-NH_3 , $LiNO_3-NH_3$ and $NaSCN-NH_3$. The results obtained for the double-stage cycle show that the $LiNO_3-NH_3$ solution operates with a COP of 0.32, in the refrigeration cycle the H_2O-NH_3 pair with a COP of 0.29 and the $NaSCN-NH_3$ solution with a COP of 0.27, when it evaporates at 15°C, condenses and absorbs refrigerant at 40°C and generates vapor at 90°C. The results are presented for double- and triple stage

absorption systems with evaporation temperatures ranging between -4° and 0°C and condensation temperatures ranging from 15°C to 45°C . Their results obtained for the double-stage heat pump cycle show that the $\text{LiNO}_3\text{-NH}_3$ solution reaches a COP of 1.32, the NaSCN-NH_3 pair a COP of 1.30 and the $\text{H}_2\text{O-NH}_3$ mixture a COP of 1.24, when it condenses and absorbs refrigerant at 50°C , evaporates at 0°C and generates vapor at 90°C . For the double- and triple-stage cycles, the results are presented for evaporation temperatures ranging between 0° and 15°C .

Oliet et al. (2007) developed general models for the design of the heat exchangers (absorber, generator, condenser and evaporator) of a prototype of an air-cooled absorption chiller of 2 kW for air-conditioning using the pair $\text{H}_2\text{O-LiBr}$. They developed an absorption machine of such characteristics to be used as a test facility for validating the results obtained from the mathematical models. The discrepancies considering the heat exchanged between numerical results and experimental data are under 15% in most cases for all these components except the condenser, where the discrepancies are higher. Their conclusions reported will lead to: (i) future improvements of the mathematical simulation models and (ii) improvements in the experimental infrastructure.

Sheng et al. (2007) analyzed an absorber which is one of the most important components of a Lithium-bromide absorption chiller (LBAC) as its absorbing characteristics directly influence the performance of the whole chiller. It has been indicated that the absorbing efficiency and cooling capacity could be improved by increasing the solution concentration.

They explained mechanism of falling film absorption on horizontal tubes; the theoretical models of falling film absorption on horizontal tubes have been established. Their results show that the cooling capacity of the LBAC varies in parabola shape of curve with the solution concentration from 52.5% to 58.5%, and that the best COP occurs at concentration of 57%.

Chua et al. (2000) developed a general thermodynamic framework for the modeling of an irreversible absorption chiller at the design point, with application to a single-stage ammonia–water absorption chiller. Component models of the chiller have been assembled so as to quantify the internal entropy production and thermal conductance (UA) in a thermodynamically rigorous formalism, which is in agreement with the simultaneous heat and mass transfer processes occurring within the exchangers.

3. MATERIAL AND METHOD

3.1. Absorption Cooling Systems

Absorption cooling systems provide cooling through an evaporation/condensation process. The main differences between conventional compression cooling systems and the absorption cooling systems are that absorption chillers usually use water rather than a standard refrigerant, they operate at lower pressure conditions rather than at moderate or high pressures, and they use heat rather than a compressor as a driving force (Hondeman 2000).

Direct comparison between these systems shows that condenser, throttling valve and the evaporator, which are found in compressor systems, are basically the same in the absorption coolers. The difference is that instead of a compressor, there are some additional components. These are the generator, solution heat exchanger, solution pump, throttling valve and the absorber. Component comparison between these systems has been shown in Figure 3.1.

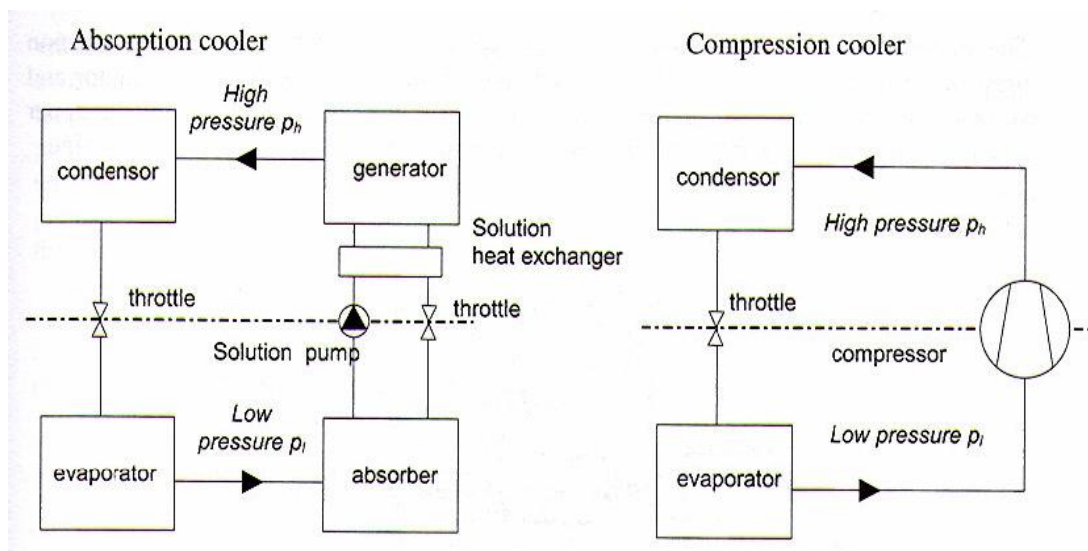


Figure 3.1. Components of the absorption cooler compared with a compression cooler (Eicker 2003)

Absorption cooling systems have certain advantages over the conventional vapor compression systems. Absorption systems use pumps instead of the compressors that are used in vapor compression systems. Since pumping a liquid to high pressures requires much less electricity than compressing a gas to the same pressure, electricity consumption is less than a vapor compression cycle. Also the refrigerant is usually water that has no damaging effect on ozone layer when compared with the chlorofluorocarbon (CFC) refrigerants used in vapor compression cycles.

During the operation, absorption cooling systems generates less noise, works on relatively low pressures and it is safer to maintain the operation with these systems. There is no large rotating component, which leads to a smaller space requirement compared to an electric chiller. The reliability of the absorption cooling systems is high, and the maintenance costs are relatively low (Eicker 2003, Hondeman 2000).

The absorption cooling systems use the high affinity between two substances. Usually the one that evaporates at a lower temperature called refrigerant while the other is called absorbent. The principle is that the system uses an absorbent liquid to attract and pull a refrigerant from the evaporator. The high affinity of the refrigerant for the absorbent causes the refrigerant to boil at a lower temperature and pressure than it normally would and transfers heat from one place to another. At the beginning of this attraction process, the concentration of the refrigerant is low so that solution has a strong attractive force on refrigerant. At this state, it is difficult to separate the refrigerant from absorbent and the solution is named to be a strong solution. While the concentration increases, the attractive forces decrease. It becomes easier to separate the refrigerant and the solution becomes a weak solution. At this state, heat is added to separate the refrigerant from the absorbent, send it to the evaporator and the cycle repeats (Lazzarin et al. 1996, Herold et al. 1996, Srihirin et al. 2001, Odabaşı 2001).

Commonly used pairs of working materials are ammonia-water and water-LiBr with ammonia and water as refrigerants and water and LiBr as solvents. The main characteristic property of the refrigerant is that its phase changes easily

between liquid and vapor. Also it is the fluid that circulates in the system, so that refrigerant should be chosen with the materials and conditions that will be used to prevent corrosion and maintain reliability. While choosing the absorbent, the main aim is that it shows a high affinity with the refrigerant. Mostly the absorbents are chosen to be lithium bromide or ammonia (Herold et al. 1996, Srihirin et al. 2001).

The possible temperature range of the absorption machines are determined by the thermodynamic properties of the refrigerants. For example, at a pressure of 10^3 kPa ammonia boils at -33°C and therefore it can be used for cooling and air conditioning. However, the refrigerant water has evaporation temperatures above 0°C and used for pure air conditioning.

One advantage of LiBr systems is that the refrigerant pressure is extremely low like 10^3 Pa at 5°C and it is favorable due to the low pump power and simple construction. Another advantage is the high boiling point distance between the refrigerant and the solvent. As a result of this, when the refrigerant is expelled from the solution, pure refrigerant vapor develops. On the other hand, the boiling point distance between water and ammonia is 133 K. So, when the refrigerant is expelled from the solution, water vapor, as well as the ammonia vapor, is produced and therefore should be separated in a rectifying column. In spite of these advantages, the major disadvantage of the LiBr systems is that it is possible for LiBr to crystallize when the refrigerant concentration in the solution drops too sharply (Eicker 2003).

3.2. Working Principle of Absorption Cooling Systems

The basic operating principle of an absorption chiller is the same as that of a conventional vapor compression chiller. Instead of the compressor in the vapor compression chiller, there are absorber, pump and generator. Arrangement of a simple absorption cooling cycle is given in Figure 3.2. Heat is given to the generator, which contains a weak solution of an absorber and a refrigerant. The refrigerant evaporates, since the attractive forces are low for a weak solution. This water vapor comes to the condenser. After condensation, it is throttled through the evaporator, and gets heat from the surrounding. After that, it turns to the absorber, in which vapor is absorbed and solution become a strong solution. After condensation, the

solution becomes a strong solution and it is pumped to the generator, so that the cycle continues (Lazzarin et al. 1996, Herold et al. 1996, Srihirin et al. 2001, Eicker 2003, Hondeman 2003).

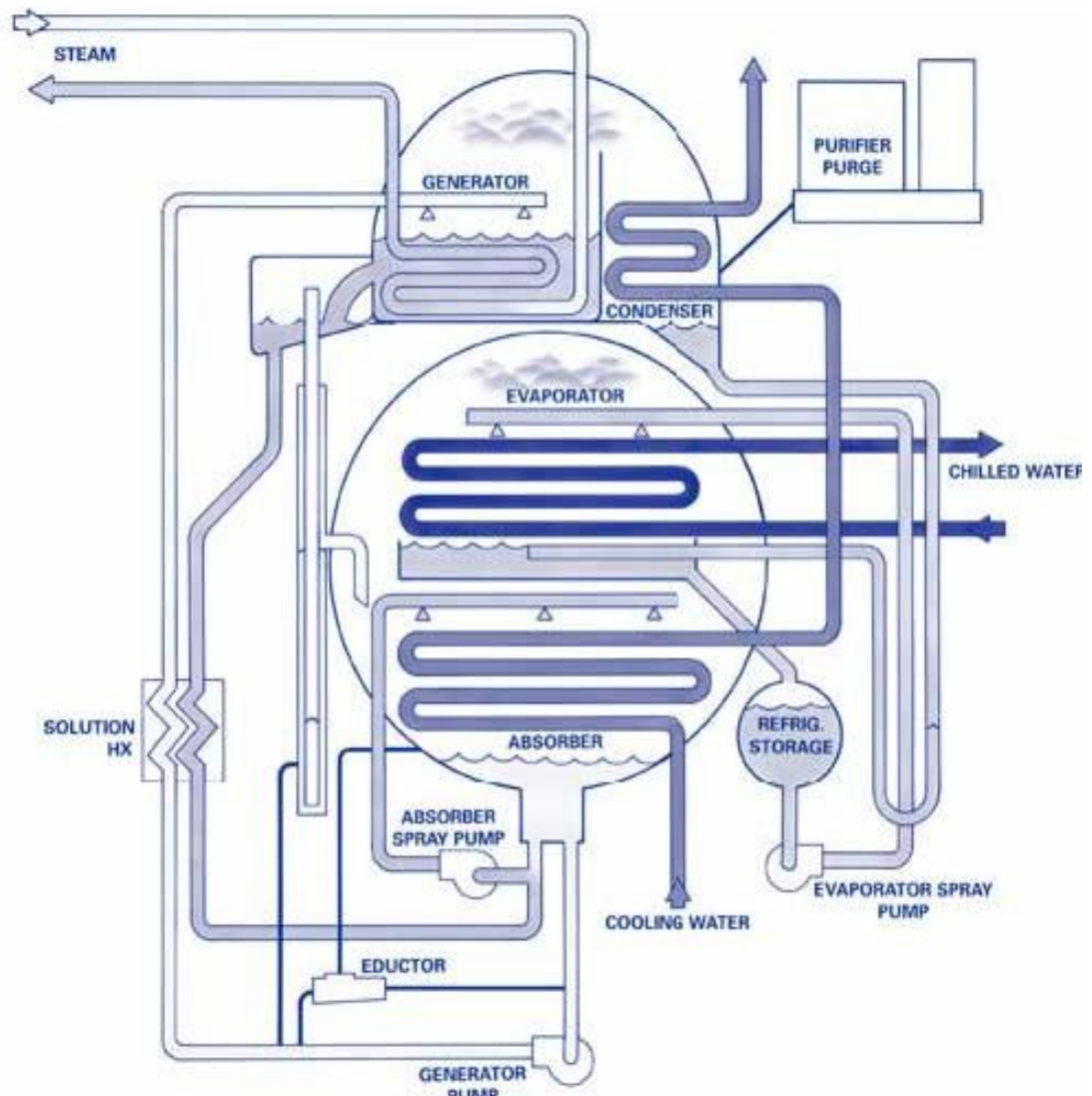


Figure 3.2. Arrangement of the components of absorption

3.3. Types of Absorption Cooling Systems

Absorption cooling systems are divided into two categories according to the heat source they use. Direct-fired systems contain a burner that runs on natural gas or another fuel to produce the heat required for the absorption process. Indirect-fired systems use steam or hot water, produced externally by a boiler or cogeneration system. Also these systems could be classified as water-cooled absorption systems and air-cooled absorption systems. Water-cooled absorption systems that are available on the market usually use water as a refrigerant and a lithium bromide solution as the absorbent, while the air-cooled absorption systems usually use ammonia as the refrigerant and water as the absorbent.

Another classification for these systems could be made according to the number of refrigeration cycles used in the system. Single-effect cooling systems use thermal energy to drive a single refrigeration cycle. Single-effect systems are usually suitable for lower temperature applications, probably around 75-132°C. Double-effect cooling systems use two refrigeration cycles. The first is driven by high temperature thermal energy and the second is driven by lower temperature energy rejected by the previous cycle's condenser. The double-effect systems require steam at around 190°C and 900 kPa. The comparison for the coefficient of performance figures for multistage absorption chillers are given in Figure 3.3 (Grossman 2002).

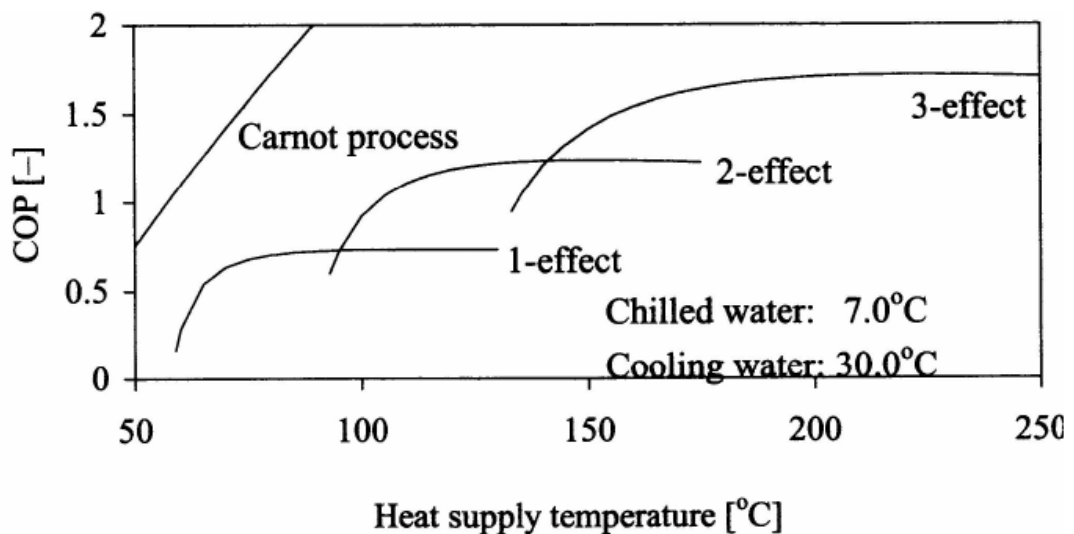


Figure 3.3. Comparison of COPs for multistage absorption chillers

3.3.1. Single effect Absorption Cooling Systems

The single-effect “cycle” refers to the transfer of fluids through the four major components of the refrigeration machine - evaporator, absorber, generator and condenser, as shown in the Pressure-Temperature diagram in Figure 3.4.

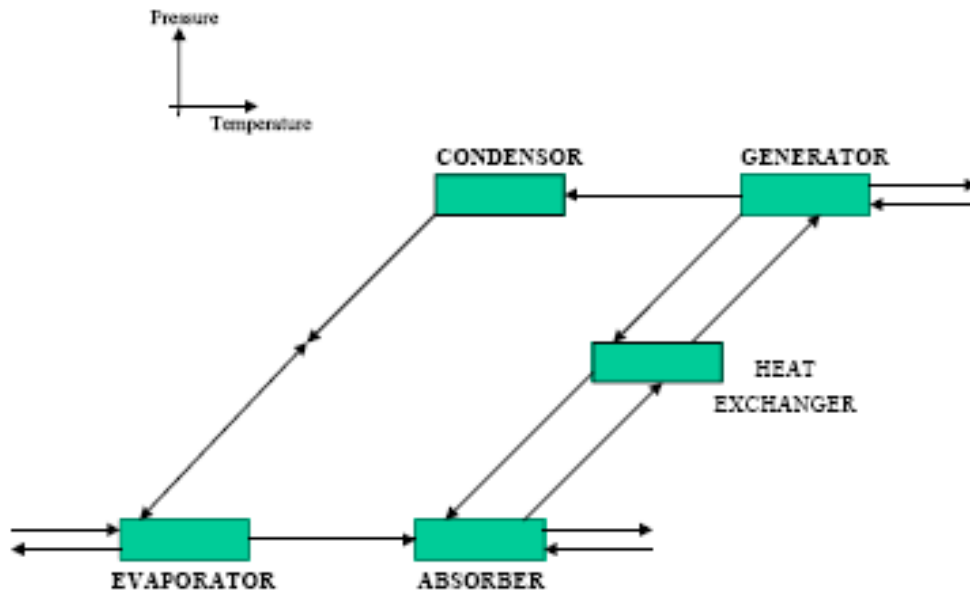


Figure 3.4. Single-effect absorption refrigeration cycle

Single-effect LiBr/H₂O absorption chillers use low pressure steam or hot water as the heat source. The water is able to evaporate and extract heat in the evaporator because the system is under a partial vacuum. The thermal efficiency of single-effect absorption systems is low.

Although the technology is sound, the low efficiency has inhibited the cost competitiveness of single-effect systems. Most new single-effect machines are installed in applications where waste heat is readily available.

3.3.2. Double effect Absorption Cooling Systems

The desire for higher efficiencies in absorption chillers led to the development of double-effect LiBr/H₂O systems. The double-effect chiller differs from the single-effect in that there are two condensers and two generators to allow for more refrigerant boil-off from the absorbent solution. Figure 3.5. shows the double effect absorption cycle on a Pressure-Temperature diagram. The higher temperature generator uses the externally supplied steam to boil the refrigerant from the weak absorbent. The refrigerant vapor from the high temperature generator is condensed and the heat produced is used to provide heat to the low temperature generator.

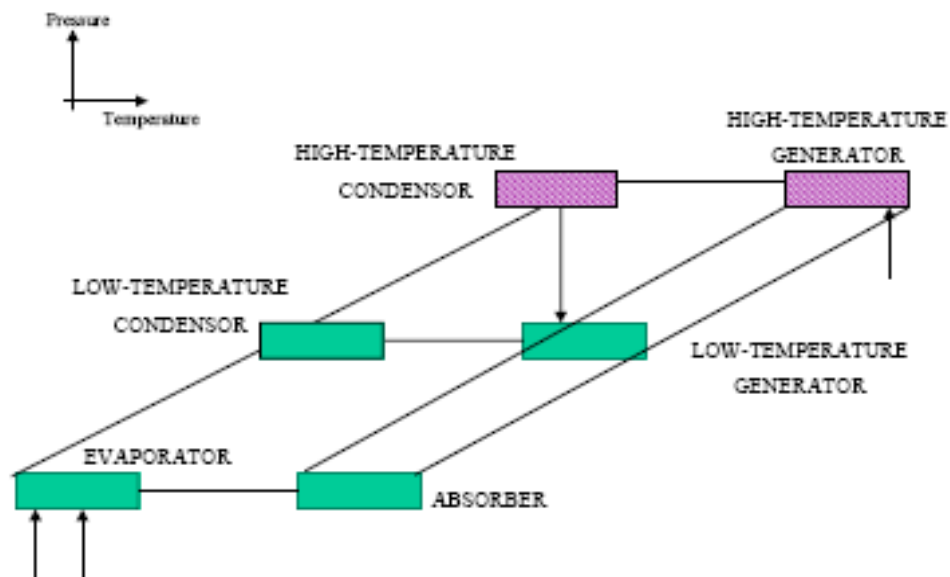


Figure 3.5. Double-effect absorption -refrigeration cycle

These systems use gas-fired combustors or high pressure steam as the heat source. Double-effect absorption chillers are used for air-conditioning and process cooling in regions where the cost of electricity is high relative to natural gas. Double-effect absorption chillers are also used in applications where high pressure steam, such as district heating, is readily available. Although the double-effect machines are more efficient than single-effect machines, they have a higher initial manufacturing cost.

3.3.3. Triple effect Absorption Cooling Systems

The triple-effect cycles are the next logical improvement over the double-effect. Triple-effect absorption chillers are under development, as the next step in the evolution of absorption technology. Figure 3.6. shows the triple effect absorption cycle on a Pressure-Temperature diagram. The refrigerant vapor from the high and medium temperature generators is condensed and the heat is used to provide heat to the next lower temperature generator. The refrigerant from all three condensers flows to an evaporator where it absorbs more heat.

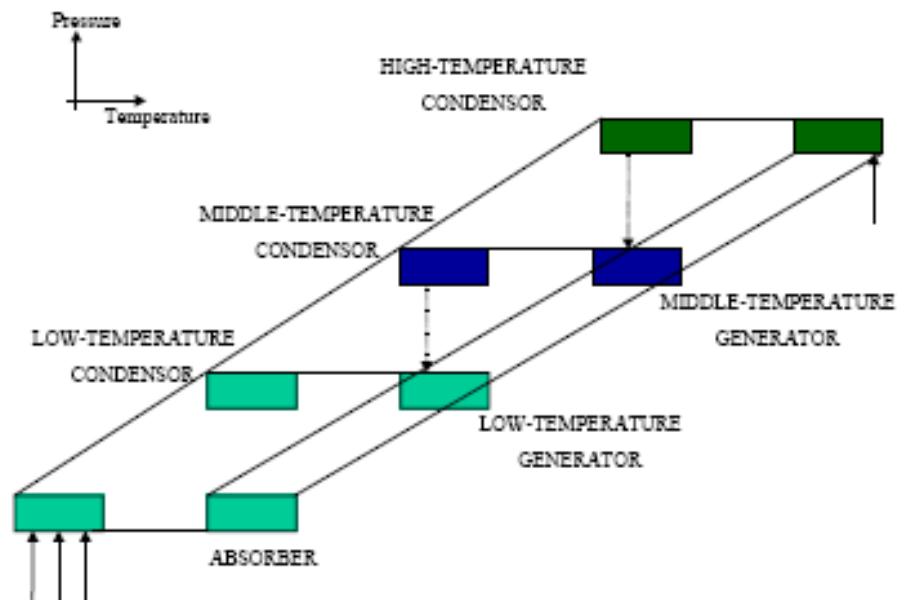


Figure 3.6. Triple-effect absorption cycle

3.3.4. Hybrid Absorption Cooling Systems

Hybrid systems capture the best of both gas and electric usage by installing an absorption system in parallel with an electric vapor compression system. In a typical hybrid system, the electricity driven chiller takes advantage of the lowest time of use costs during off-peak hours.

The absorption chiller is used as the primary source during the on-peak hours, with the vapor compression chiller used for the remainder of the load, as needed. The specifics of any hybrid system design depend on the nature of the cooling load, and

the characteristics of the local gas and electric rates, but there are many applications where a hybrid system is advantageous. This is especially true for large facilities with sophisticated energy management personnel who can optimize system performance and energy costs. The hybrid plant crystallizes the concept of a system design that maximizes the flexibility of “time dependent” energy selection. The use of absorption chillers eliminates the high incremental cost of electricity. The hybrid approach will play a larger role in cooling options as utility rate structures continue to be more variable.

3.4. Advantages of Absorption Cooling Systems

The primary energy benefit of gas cooling systems is reduction in operating costs by avoiding peak electric demand charges and time-of-day rates. The use of gas absorption chillers eliminates the high incremental cost of electric cooling. The restructuring of the electric utility industry adds significant complexity and uncertainty to the HVAC design and operation. The key is operational flexibility.

Gas cooling systems eliminate some of the variability associated with electric rate structures, while a hybrid system maximizes the flexibility of an “all- energy” plant. Natural gas cooling systems have greater resource efficiency than similar electric systems.

A direct-fired absorption system can supply hot water in addition to chilled water if:

- equipped with an auxiliary heat exchanger
- the hot water circuit of the auxiliary heat exchanger includes the necessary control devices.

If the equipment is to provide heating as well as cooling, then a true comparison of equipment cost and annual maintenance costs between an electric and gas system must consider the electric centrifugal chiller plus a boiler. The results of such a comparison should show the direct-fired absorption chiller annualized costs, including maintenance, operating, and first costs, to be less than or roughly equal to those of an electric chiller and boiler.

3.5. Absorption Cooling Applications

The primary variable that drives the economics of gas absorption cooling is the electric demand charge. Ideal candidates for gas absorption applications are those where the peak demand charge is high. Since cooling is generally the primary cause of sharp spikes in a building's electric load profile, it is advantageous to investigate alternatives that can reduce this peak. Gas cooling minimizes or flattens the electric peaks in a building's electric load.

The absorption cooling system should be operated to maximize electric peak-shaving in areas with high demand charges or extended daytimes and evenings electricity rates. Hybrid systems, which use an electric chiller for base load, and the gas engine-driven chiller for peak load, are an attractive option in regions with high electric costs. Gas absorption chillers can be economically installed as a cooling only system, or as part of an integrated cooling and heating facility.

In many parts of the country, the cost difference between electricity and natural gas is sufficient to justify absorption chillers. Additional cost savings can be realized through the use of heat recovery.

In summary, good applications for absorption chillers have the following characteristics:

- High demand charges
- Coincident need for air conditioning and heating
- Maintenance and service requirements are acceptable to building owner

3.6. Absorption Cooling Systems with Natural Gas

Natural gas is a combustible gas that is a mixture of simple hydrocarbon compounds. It is a fossil fuel that contains primarily methane, along with small amounts of ethane, butane, pentane, and propane. Natural gas does not contain carbon monoxide. The by products of burning natural gas are primarily carbon dioxide and water vapor, making natural gas safer for our environment compared with the use of other fossil fuels.

Natural gas is a colorless, tasteless, odorless, and non-toxic gas. Because it is odorless, a powerful chemical called mercaptan is added to the gas, in very small amounts, to give the gas a distinctive smell of rotten eggs. This strong smell can be helpful in detecting the source of any gas leak. Natural gas is about 40% lighter than air, so should it ever leak, it can dissipate into the air. Other positive attributes of natural gas are a high ignition temperature and a narrow flammability range, meaning natural gas will ignite at temperatures above 1,100⁰C degrees and burn at a mix of 4 – 15% volume in air.

Figure 3.7. shows that the electricity-natural gas consumption presentation. In summer months, the electricity consumption increase, however the natural gas consumption decreases simultaneously.

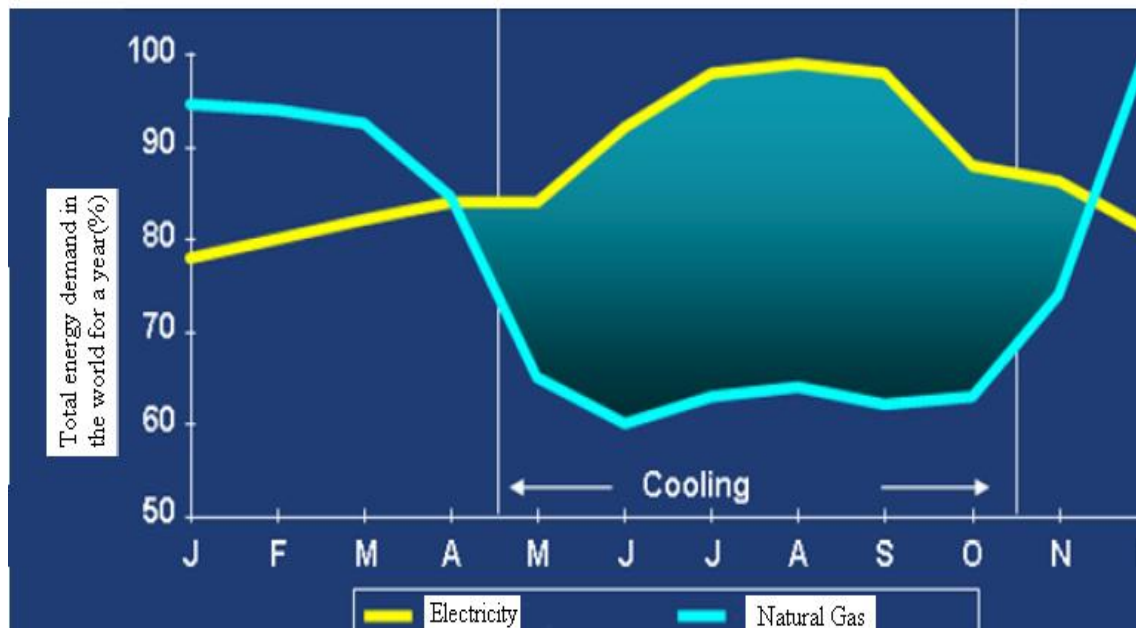


Figure 3.7. Electricity and natural gas consumption presentation

3.7. Description of Absorption Cooling System Studied

Figure 3.8. shows a double-effect direct-fired absorption chiller. Double effect means that there are two generators. Direct fired means that gas is directly fired at the generator instead of using steam or hot water. A single-effect absorption chiller using steam as the heat input to its single generator has a COP only from 0,7

to 0,8 , whereas a double-effect direct-fired absorption chiller has a COP approximately 1-1,5 and therefore is the most widely used absorption chiller. The refrigeration capacity of double-effect direct-fired absorption chillers varies from 350 to 5275 kW. A double-effect direct-fired absorption chiller mainly consists of the following components and controls:

Evaporator; an evaporator is comprised of a tube bundle, spray nozzles, a water trough, a refrigerant pump, and an outer shell. Chilled water flows inside the tubes. A refrigerant pump sprays the liquid refrigerant over the outer surface of the tube bundle for a higher rate of evaporation. A water trough is located at the bottom to maintain a water level for recirculation.

Absorber; in an absorber, there are tube bundles in which cooling water flows inside the tubes. Solution is sprayed over the outer surface of the tube bundle to absorb the water vapor. A solution pump is used to pump the diluted solution to the heat exchanger and low-temperature generator.

Heat exchangers; there are two heat exchangers: low-temperature heat exchanger in which the temperature of hot concentrated solution is lower and high-temperature heat exchanger in which the temperature of hot concentrated solution is higher. In both heat exchangers, heat is transferred from the hot concentrated solution to the cold diluted solution. Shell-and-tube or plate-and-frame heat exchangers are most widely used for their higher effectiveness.

Generators; are also called desorbers. In the direct-fired generator, there are the fire tube, flue tube, vapor/liquid separator, and flue-gas economizer. Heat is supplied from the gas burner or other waste heat source. The low-temperature generator is often of the shell-and-tube type. The water vapor vaporized in the direct-fired generator is condensed inside the tubes. The latent heat of condensation thus released is used to vaporize the dilute solution in the low temperature generator.

Condenser; a condenser is usually also of the shell-and-tube type. Cooling water from the absorber flows inside the tubes. Throttling devices, orifices and valves are often used as throttling devices to reduce the pressure of refrigerant and solution to the required values.

Air purge unit; is used to remove these non-condensable gases from the chiller. A typical air purge unit is comprised of a pickup tube, a purge chamber, a solution spray, cooling water tubes, a vacuum pump, a solenoid valve, and a manual shut-off valve.

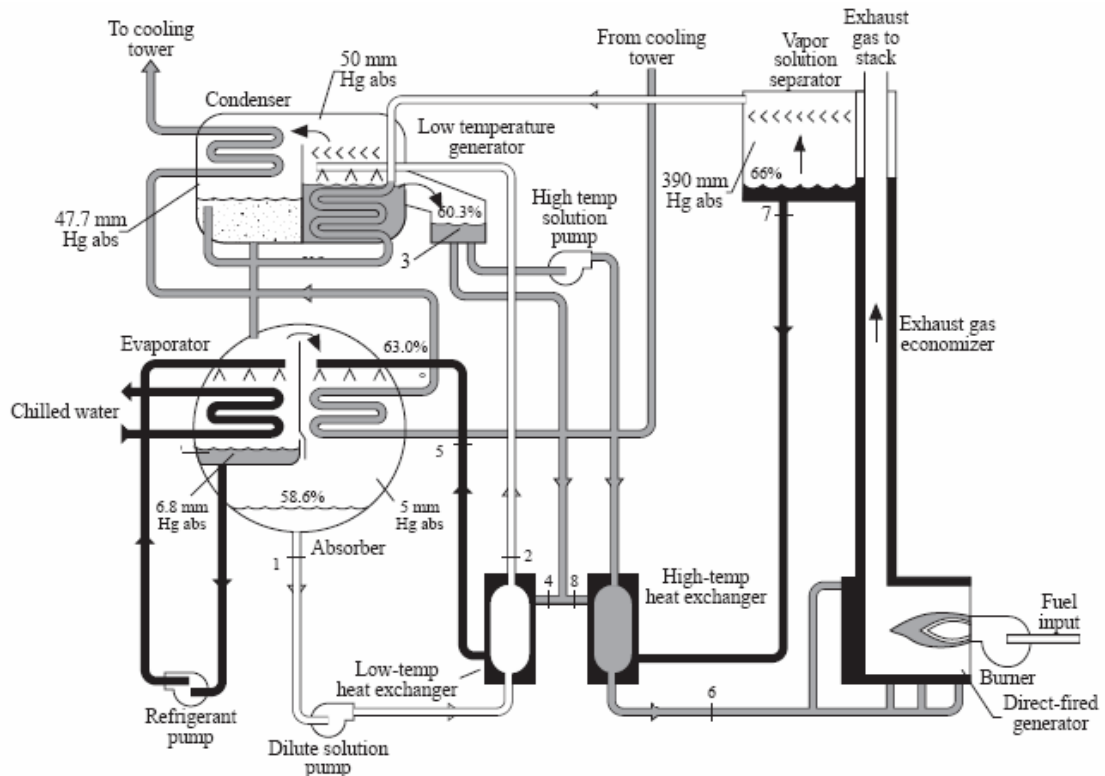


Figure 3.8.A double effect direct fired absorption chiller schematic diagram

When non-condensable gases leak into the system, they tend to migrate to the absorber where pressure is lowest. Non-condensable gases and water vapor are picked from the absorber through the pickup tube. Water vapor is absorbed by the solution spray and returned to the absorber through a liquid trap at the bottom of the purge chamber. Heat of absorption is removed by the cooling water inside the tubes.

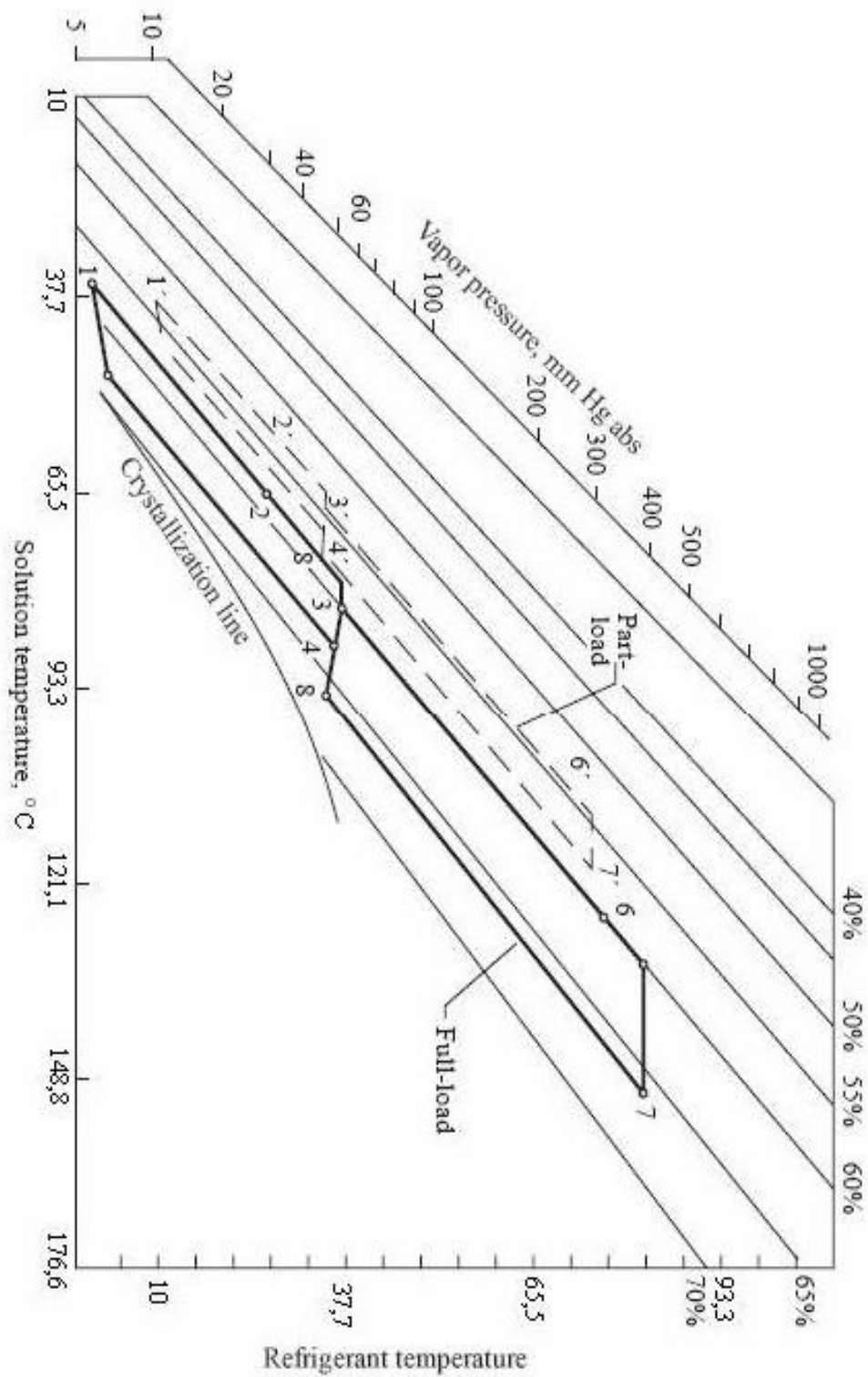


Figure 3.9. A double Effect Direct Fired Absorption Cycle

An absorption cycle shows the properties of the solution and its variation in concentrations, temperature, and pressure during absorbing, heat exchanging, and concentration processes on an equilibrium chart as shown in Figure 3.9. The ordinate of the equilibrium chart is the saturated temperature and pressure of water vapor, in °C and mm Hg abs. The abscissa is the temperature of the solution, in °C. Concentration lines are incline lines. At the bottom of the concentration lines, there is a crystallization line or saturation line. If the mass fraction of LiBr in a solution which remains at constant temperature is higher than the saturated condition, that part of LiBr exceeding the saturation condition tends to form solid crystals.

Because there are two generators, the flow of solution from the absorber to generators can be in series flow, parallel flow, or reverse-parallel flow. In a series-flow system, the diluted solution from the absorber is first pumped to the direct-fired generator and then to the low-temperature generator. In a parallel-flow system, diluted solution is pumped to both direct-fired and low-temperature generators in parallel.

In a reverse-parallel-flow system as shown in Figure 3.8, diluted solution is first pumped to the low temperature generator. After that, the partly concentrated solution is then sent to the direct-fired generator as well as to the intermediate point 4 between high- and low-temperature heat exchangers in parallel. At point 4, partly concentrated solution mixes with concentrated solution from a direct-fired generator. A reverse-parallel-flow system is more energy efficient.

In a typical double-effect direct-fired reverse-parallel-flow absorption chiller operated at design full load, water is usually evaporated at a temperature of 7°C and a saturated pressure of 6.8 mm Hg abs in the evaporator. Chilled water returns from the AHUs or fan coils at a temperature typically 12°C, cools, and leaves the evaporator at 12°C. A refrigeration effect is produced due to the vaporization of water vapor and the removal of latent heat of vaporization from the chilled water.

Water vapor in the evaporator is then extracted to the absorber due to its lower vapor pressure. It is absorbed by the concentrated LiBr solution at a pressure of about 5 mm Hg abs. After absorption, the solution is diluted to a concentration of 58.6% and its temperature increases to 35°C (point 1). Most of the heat of absorption

and the sensible heat of the solution are removed by the cooling water inside the tube bundle. Diluted solution is then pumped by a solution pump to the low-temperature generator through a low-temperature heat exchanger.

In the low-temperature generator, the dilute solution is partly concentrated to 60.3% at a solution temperature of 110°C (point 3). It then divides into two streams: one of them is pumped to the direct fired generator through a high-temperature heat exchanger, and the other stream having a slightly greater mass flow rate is sent to the intermediate point 4. In the direct-fired generator, the concentrated solution leaves at a concentration of 66% and a solution temperature of 140°C (point 7). The mixture of concentrated and partly concentrated solution at point 4 has a concentration of 63% and a temperature of 89°C. It enters the low-temperature heat exchanger. Its temperature drops to 50°C before entering the absorber (point 5).

In the direct-fired generator, water is boiled off at a pressure of about 390 mm Hg abs. The boiled-off water vapor flows through the submerged tube in the low-temperature generator. The release of latent heat of condensation causes the evaporation of water from the dilution solution at a vapor pressure of about 50 mm Hg abs.

The boiled-off water vapor in the low-temperature generator flows to the condenser through the top passage and is condensed into liquid water at a temperature of about 37°C and a vapor pressure of 47.7 mm Hg abs. This condensed liquid water is combined with the condensed water from the submerged tube at the trough. Both of them return to the evaporator after its pressure is throttled by an orifice plate.

3.8. Cooling Load Profile of Air Conditioning Place

In this study, a place is planned in Çukurova Region for the air conditioning by the absorption cooling. All of the heat losses are added the total cooling loads. In this section, cooling load of the place was calculated using the Artificial Neural Network (ANN) model. A MS-Excel worksheet was prepared for the calculations.

Calculations were performed for all days of a year, which is considered as the design data for Çukurova Region. The outdoor design parameter for Adana (Çukurova Region) is hourly temperature data throughout a year.

3.9. Description of Artificial Neural Network (ANN) model

The best example of a neural network is probably the human brain. In fact, the human brain is the most complex and powerful structure known today. Artificial neural Networks are composed of simple elements operating in parallel. These elements are inspired by biological nervous systems. The ANN modeling is carried out in two steps; the first step is to train the network whereas the second is to test the network with data, which were not used for training. The unit element of an ANN is the neuron (node). As in nature, the network function is determined largely by the connections between the elements. Figure 3.10. illustrates how information is processed through a single node. The node receives weighted activation from other nodes through its coming connections. First, these are added (summation function). The result is then passed through an activation function, the outcome being the activation of the node. For each of the outgoing connections, this activation value is multiplied with the specific weight and transferred to the next node.

A training set is a group of matched input and output patterns. This is used for the training of the network, usually by suitable adaptation of the synaptic weights. The outputs are the dependent variables that the network produces for the corresponding input. It is important that all the information the network needs to learn is supplied to the network as a data set. When each pattern is read, the network uses the input data to produce an output, which is then compared to the training pattern, i.e. the correct or desired output. If there is a difference, the connection

weights (usually but not always) are altered in such a direction that the error is decreased. After the network has run through all the input patterns, if the error is still greater than the maximum desired tolerance, the ANN runs through all the input patterns repeatedly until all the errors are within the required tolerance. When the training reaches a satisfactory level, the network holds the weights constant and the trained network can be used to make decisions, identify patterns, or define associations in new input data sets not used to train it.

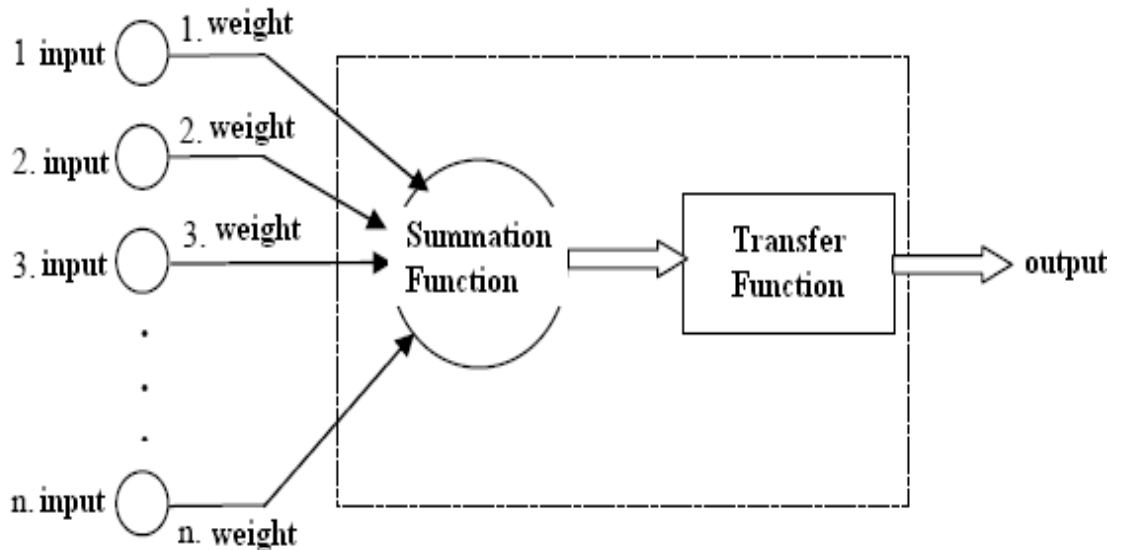


Figure 3.10. Information for processing artificial neural network unit

3.10. Modeling of the thermodynamic properties with ANN

An absorption system consists of the evaporator, generator, condenser, absorber, solution pump, solution heat exchanger and expansion valve. A schematic representation of the absorption cycle is given in Figure 3.11. The energy and mass balance equations of the various components of an absorption system are given in Table 3.1.

The cooling coefficient of performance (COP) of the absorption system is defined as the heat load in the evaporator per unit of heat load in the generator and can be written as:

$$COP = \frac{Q_E}{Q_G} \quad (3.1)$$

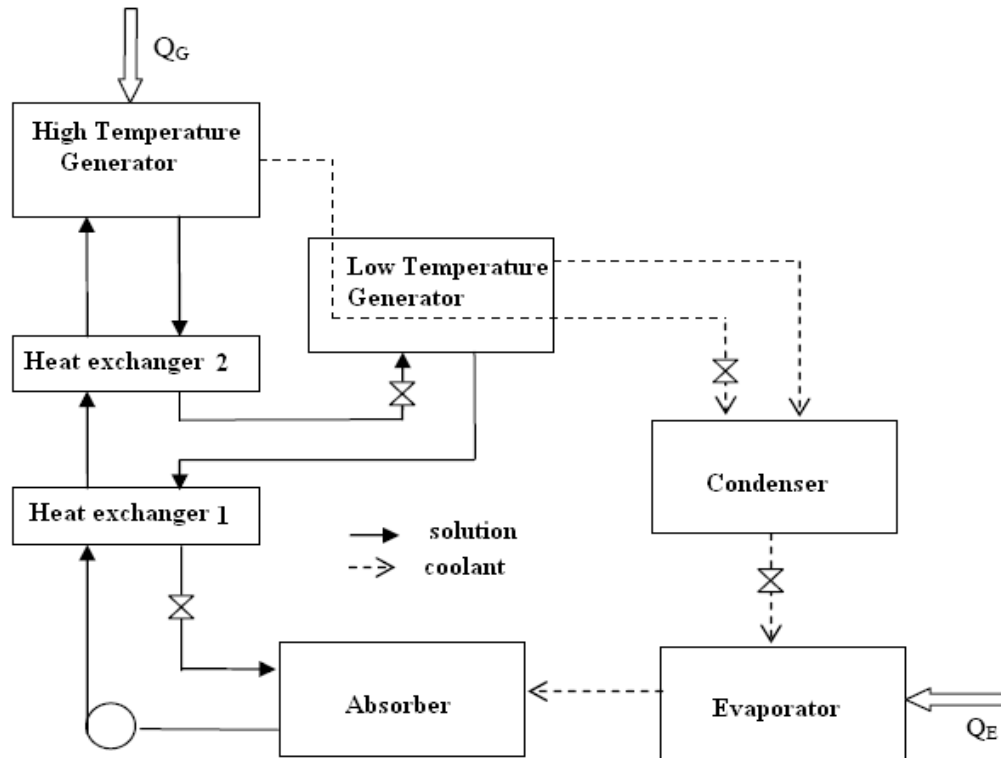


Figure 3.11. Schematic representation of the absorption cooling system

Table 3.1. Energy-mass balance equations of absorption system components

System components	Mass balance equations	Energy balance equations
Pump	$\dot{m}_1 = \dot{m}_2; x_1 = x_2$	$W = \dot{m}_2 h_2 - \dot{m}_1 h_1$
Solution heat exchanger	$\dot{m}_2 = \dot{m}_3, \dot{m}_4 = \dot{m}_5; x_2 = x_3, x_4 = x_5$	$\dot{m}_2 h_2 + \dot{m}_4 h_4 = \dot{m}_3 h_3 + \dot{m}_5 h_5$
Solution expansion valve	$\dot{m}_5 = \dot{m}_6; x_5 = x_6$	$h_5 = h_6$
Absorber	$\dot{m}_1 = \dot{m}_6 + \dot{m}_{10}; \dot{m}_1 x_1 = \dot{m}_6 x_6 + \dot{m}_{10} x_{10}$	$Q_A = \dot{m}_6 h_6 + \dot{m}_{10} h_{10} - \dot{m}_1 h_1$
Generator	$\dot{m}_3 = \dot{m}_4 + \dot{m}_7; \dot{m}_3 x_3 = \dot{m}_4 x_4 + \dot{m}_7 x_7$	$Q_G = \dot{m}_4 h_4 + \dot{m}_7 h_7 - \dot{m}_3 h_3$
Condenser	$\dot{m}_7 = \dot{m}_8; x_7 = x_8$	$Q_K = \dot{m}_7 h_7 - \dot{m}_8 h_8$
Refrigerant expansion valve	$\dot{m}_8 = \dot{m}_9; x_8 = x_9$	$h_8 = h_9$
Evaporator	$\dot{m}_9 = \dot{m}_{10}; x_9 = x_{10}$	$Q_E = \dot{m}_{10} h_{10} - \dot{m}_9 h_9$

The parameters and temperature intervals of double effect absorption system are given in Table 3.2.

Table 3.2. Parameters and temperature intervals of absorption system

High temperature generator, T_{Gh}	85-180 ⁰ C
Low temperature generator, T_{Gl}	60-115 ⁰ C
Evaporator temperature, T_E	2-14 ⁰ C
Condenser temperature, T_C	30-50 ⁰ C
Absorber temperature, T_A	30-50 ⁰ C
Heat exchanger 1 efficiency η_1	0,8
Heat exchanger 2 efficiency η_2	0,85

The first equation for calculation of ANN, Root Mean Squared (RMS) can be written as;

$$RMS = \sqrt{\frac{\sum_{m=1}^n (y_{p,m} - t_{m,m})^2}{n}} \quad (3.2)$$

Also absolute permutation percentage (R^2) and permutation coefficient (cov) can be defined as following;

$$R^2 = 1 - \frac{\sum_{m=1}^n (t_{m,m} - y_{p,m})^2}{\sum_{m=1}^n (t_{m,m} - \bar{t}_{m,m})^2} \quad (3.3)$$

$$cov = \frac{RMS}{|\bar{t}_{m,m}|} \times 100 \quad (3.4)$$

In this equations, n is number of data, $y_{p,m}$ is estimated value, $t_{m,m}$ is real value and $\bar{t}_{m,m}$ is all real value implied.

In this study, the back-propagation learning algorithm is used in a feed-forward, single hidden layer network. Logistic sigmoid transfer function is used as the activation function for both the hidden layer and the output layer. The transfer function used is presented in Equation (3.5). The values of the training and test data

were normalized to a range of 0–1. Levenberg–Marquardt (LM) Back Propagation training was repeatedly applied until satisfactory training is achieved.

$$F(z) = \frac{1}{1 + e^{-z}} \quad (3.5)$$

In that equation, z is the weighted sum of the input.

The computer program was performed under MATLAB environment using the neural network toolbox. The data set for the COP available included 150 data patterns. From these 120 data patterns were used for the training of the network and the remaining 30 patterns were randomly selected and used as test data set.

Figure 3.12. shows the architecture of the ANN used for COP prediction. In this figure, the temperature is the input data and COP is the actual output.

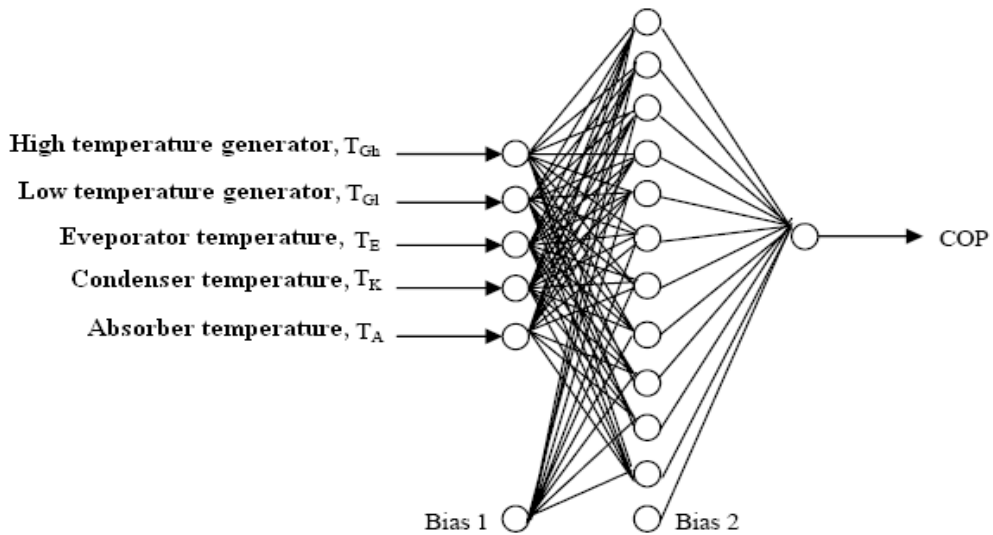


Figure 3.12. ANN model used for COP prediction

Table 3.3. shows that the best appraisalment is single hidden layer network and eleven neurons provide. The configuration LM-11 appeared to be the most optimal topology for this application in Table 3.3.

The coefficient of multiple determination (R²-value) obtained is 0.9939 which is very satisfactory.

Table 3.3. Statistical results of thermodynamic properties with ANN

Algorithm neuron	RMS	cov	R2
LM-3	0.077248	0.050841	0.7871
LM-4	0.107283	0.070608	0.5894
LM-5	0.059456	0.039131	0.8739
LM-6	0.046839	0.030827	0.9217
LM-7	0.053005	0.034886	0.8997
LM-8	0.113569	0.074746	0.5399
LM-9	0.055837	0.03675	0.8887
LM-10	0.041313	0.02719	0.9391
LM-11	0.012988	0.008548	0.9939
LM-12	0.065688	0.039008	0.8416
LM-13	0.067092	0.044157	0.8394
SCG-3	0.112051	0.073747	0.5521
SCG-4	0.091771	0.0604	0.6995
SCG-5	0.096069	0.063228	0.6707
SCG-6	0.098975	0.05791	0.6846
SCG-7	0.103374	0.068036	0.6188
SCG-8	0.108034	0.071103	0.5836
SCG-9	0.10075	0.063479	0.6100
SCG-10	0.101338	0.066696	0.6336
SCG-11	0.10012	0.05529	0.6485
SCG-12	0.121792	0.080158	0.4709
SCG-13	0.118298	0.077858	0.5008

Mathematical formulations derived from the ANN model are presented here. In the following formulas the coefficients of the input parameters are used to evaluate the E_i (summation function of neuron i) and F_i (activation function of neuron i). These coefficients represent the weight values of the summation function of each neuron belonging to the hidden layer of the trained network.

Table 3.3. gives some values for calculations of COP which derived by following mathematical formulations.

$$T_E = t_E / 15 \quad (3.6)$$

$$T_A = t_A / 51 \quad (3.7)$$

$$T_C = t_C / 51 \quad (3.8)$$

$$T_{Gh} = t_{Gh} / 181 \quad (3.9)$$

$$T_{Gi} = t_{Gi} / 115 \quad (3.10)$$

Equations (3.6 - 3.10) are used for normalize the temperature values.

$$E_1 = 2.5389 T_E - 7.902 T_A + 2.7454 T_C + 8.4139 T_{Gh} - 16.1867 T_{Gl} + 6.2155 \quad (3.11)$$

$$F_1 = \frac{1}{1 + e^{-E_1}} \quad (3.12)$$

$$E_2 = 12.3617 T_E - 24.4423 T_A + 0.31346 T_C + 6.7826 T_{Gh} - 9.2802 T_{Gl} + 22.0959 \quad (3.13)$$

$$F_2 = \frac{1}{1 + e^{-E_2}} \quad (3.14)$$

$$E_3 = 2.2282 T_E - 6.0043 T_A - 15.0899 T_C - 10.1824 T_{Gh} - 7.6807 T_{Gl} + 19.2814 \quad (3.15)$$

$$F_3 = \frac{1}{1 + e^{-E_3}} \quad (3.16)$$

$$E_4 = 6.5151 T_E - 23.6904 T_A - 12.6504 T_C + 18.0498 T_{Gh} + 14.3751 T_{Gl} + 6.7257 \quad (3.17)$$

$$F_4 = \frac{1}{1 + e^{-E_4}} \quad (3.18)$$

$$E_5 = -6.4267 T_E + 21.766 T_A - 13.9398 T_C - 18.818 T_{Gh} - 15.2468 T_{Gl} - 5.4591 \quad (3.19)$$

$$F_5 = \frac{1}{1 + e^{-E_5}} \quad (3.20)$$

$$E_6 = -107.7234 T_E - 107.2935 T_A - 163.7942 T_C + 140.7863 T_{Gh} + 153.0092 T_{Gl} + 63.7153 \quad (3.21)$$

$$F_6 = \frac{1}{1 + e^{-E_6}} \quad (3.22)$$

$$E_7 = 2.1712 T_E - 4.6574 T_A - 1.4764 T_C + 3.559 T_{Gh} - 0.85682 T_{Gl} + 4.7089 \quad (3.23)$$

$$F_7 = \frac{1}{1 + e^{-E_7}} \quad (3.24)$$

$$E_8 = -1.8713 T_E + 6.0763 T_A - 5.8244 T_C + 5.0303 T_{Gh} + 5.6849 T_{Gl} - 5.203 \quad (3.25)$$

$$F_8 = \frac{1}{1 + e^{-E_8}} \quad (3.26)$$

$$E_9 = 4.746 T_E + 22.3984 T_A - 1.9679 T_C - 10.2601 T_{Gh} + 17.1526 T_{Gl} - 23.8604 \quad (3.27)$$

$$F_9 = \frac{1}{1 + e^{-E_9}} \quad (3.28)$$

$$E_{10} = -108.9605 T_E - 111.2968 T_A - 171.2557 T_C + 151.6227 T_{Gh} + 143.6143 T_{Gl} + 72.143 \quad (3.29)$$

$$F_{10} = \frac{1}{1 + e^{-E_{10}}} \quad (3.30)$$

$$E_{11} = -3.1318 T_E + 9.2264 T_A + 0.28507 T_C + 14.678 T_{Gh} + 25.3457 T_{Gl} - 26.7879 \quad (3.31)$$

$$F_{11} = \frac{1}{1 + e^{-E_{11}}} \quad (3.32)$$

$$E_{12} = 12.9149 F_1 - 0.873298 F_2 + 5.7019 F_3 - 12.6376 F_4 - 40.6315 F_5 + 58.7494 F_6 + 14.9586 F_7 + 14.1867 F_8 - 0.34107 F_9 - 58.7162 F_{10} + 1.0235 F_{11} - 13.3665 \quad (3.33)$$

Double effect absorption cooling system compute COP (with Equations of 3.11 – 3.33 and depend of system components temperature values) with the following equation;

$$F_{12} = COP = \left(\frac{1}{1 + e^{-E_{12}}} \right) \times 1.74 \quad (3.34)$$

In Table 3.4. a comparison is presented between the actual COP predicted with the equations derived from ANN for absorption cooling system. As can be seen in most of the cases the error is well within acceptable limits.

Table 3.4. COP values of absorption cooling systems compared with the real and calculated with ANN

T_E	T_A	T_C	T_{G1}	T_{Gh}	Real COP values	Approximate COP with ANN	error
2	30	30	75,7	118,4	1,652	1,651	0,001
2	30	40	81,4	122,2	1,592	1,586	0,006
2	30	50	92,5	134,5	1,573	1,569	0,004
2	40	30	74,3	121,6	1,259	1,255	0,004
2	40	40	85,3	133,9	1,211	1,207	0,004
2	40	50	107,7	164,5	1,529	1,529	0,000
2	50	40	98,5	160,7	1,27	1,27	0,000
6	30	40	72,6	105,8	1,546	1,557	-0,011
6	30	40	98,4	145,5	1,724	1,722	0,002
6	30	50	102,4	147,1	1,724	1,72	0,004
6	40	30	84,3	135,2	1,605	1,604	0,001
6	50	30	82,4	137,7	1,342	1,347	-0,005
6	50	50	101,7	157,7	1,033	1,038	-0,005
10	40	40	77,8	117,1	1,46	1,456	0,004
10	40	40	100,5	152,7	1,666	1,662	0,004
10	40	50	111,7	165,1	1,672	1,668	0,004
10	50	30	91,6	150,1	1,554	1,559	-0,005
10	50	40	98,6	155,9	1,536	1,536	0,000
14	40	30	68,9	105,7	1,685	1,68	0,005
14	40	40	74	108,5	1,567	1,57	-0,003
14	40	50	111,7	161,9	1,717	1,714	0,003
14	50	40	92,5	143,6	1,57	1,572	-0,002
14	50	50	94,1	140,6	1,331	1,32	0,011
14	50	50	108,6	164	1,595	1,592	0,003

Table 3.4. shows that ANN calculated COP values are very similar to the real COP values. The ANN calculated are COP results considerably close to the real COP values and this shows the ANN method is applicable truly.

3.11. Description of Vapor Compression Cooling Systems

A refrigerator is a machine that removes heat from a low temperature region. Since energy cannot be destroyed, the heat taken in at a low temperature must be dissipated to the surroundings.

The most common refrigeration system in use today involves the input of work (from a compressor) and uses the vapor compression cycle. In a vapor compression refrigeration system a gas is alternatively compressed and expanded and goes from the liquid to the vapor state. The basic components of a vapor-compression refrigeration system are shown below in Figure 3.13.

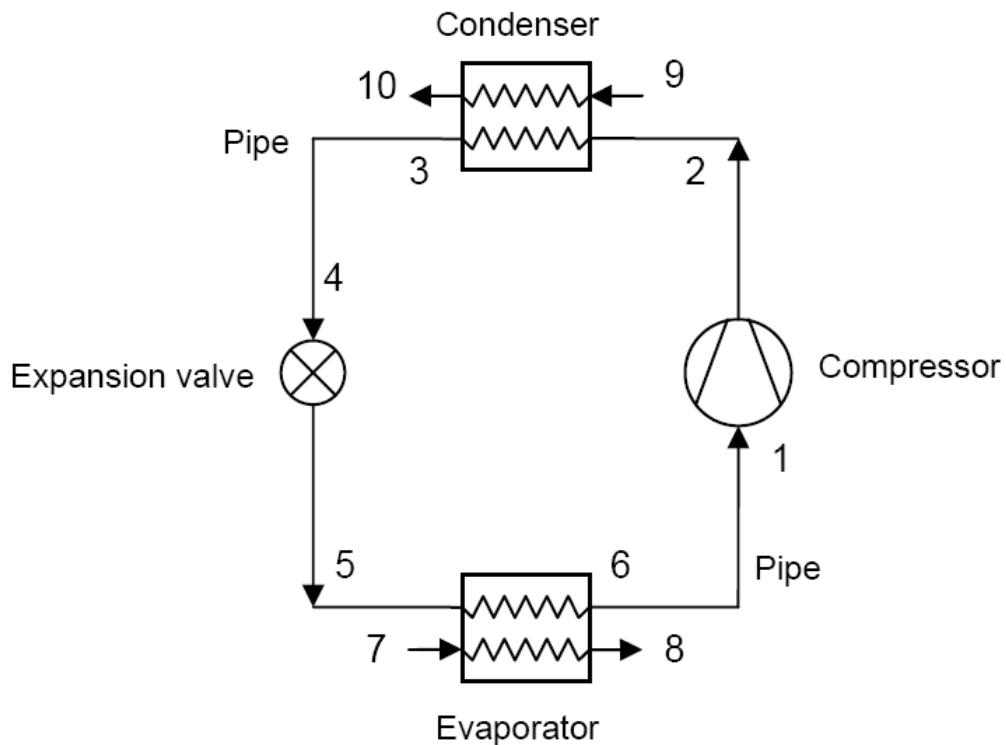


Figure 3.13. Layout of the vapor compression refrigeration system

Refrigerant vapor enters a compressor at a slightly superheated state (1) and is then compressed to state 2. From 2 to high pressure high temperature vapor is first sensibly cooled to saturation, then condensed and ultimately sub-cooled to state 3. From 3 to 4 the liquid refrigerant flows to the inlet of expansion valve in an adiabatic process. From 5 to 6 all the liquids in the evaporator and then slightly superheated to

state 6. From there the vapor refrigerant flows through a tube to the inlet of the compressor (1) to close the system. As a result, heat is transferred from the refrigerated section to the refrigerant (i.e. heat is absorbed by the refrigerant) causing it to pass from the liquid or near-liquid state to the vapor state again (hence the term evaporator).

The four basic components of the vapor compression refrigeration system are thus:

1. Evaporator - Heat is absorbed to boil the liquid at a low temperature, therefore a low pressure must be maintained in this section.

2. Compressor - The compressor does work on the system increasing the pressure from that existing in the evaporator (drawing in low- pressure, low-temperature saturated vapor) and to that existing in the condenser (i.e., delivering high pressure and high temperature vapor to the condenser.

3. Condenser - The high pressure, high temperature (superheated or saturated) vapor that enters the condenser has heat removed from it and as results it is condensed back into a liquid phase.

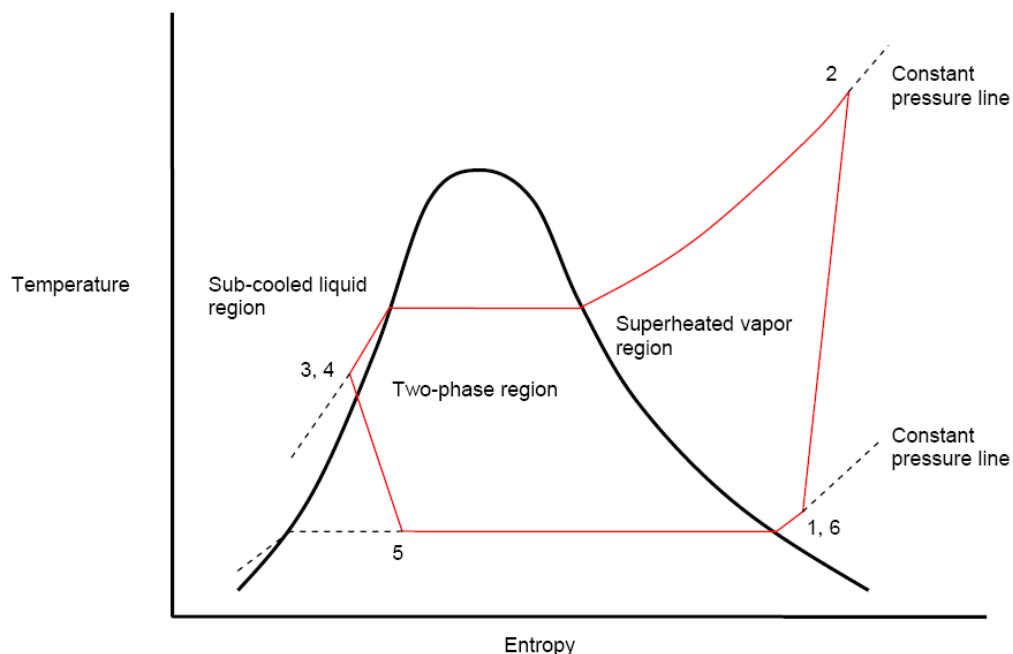


Figure 3.14. Temperature- Entropy diagram for vapor compression system

4. Expansion valve - The high pressure liquid from the condenser is expanded through this valve, allowing its pressure to drop to that existing in the evaporator.

The refrigerant then again passes to the compressor in which its pressure is again increased and the whole cycle is repeated. This cycle showed the figure 3.14.

3.12. Vapor Compression Cooling Cycle Analysis

Figure 3.14.given this information's;

1 → 2 Isentropic compression through compressor

2 → 3 Constant pressure heat removal in the condenser

3 → 4 Constant enthalpy through expansion valve

4 → 1 Constant pressure heat addition in the evaporator

In the analyses, each component is first separately considered. The evaporator, in which the desired refrigeration effect is achieved, will be considered first. As the refrigerant passes through the evaporator, heat transfer from the refrigerated space results in the vaporization of the refrigerant.

Considering a control volume enclosing the refrigerant side of the evaporator, conservation of mass and energy applied to this control volume together give the rate of heat transfer per unit mass of refrigerant flow in the evaporator as:

$$\frac{\dot{Q}_{in}}{\dot{m}} = h_1 - h_4 \quad (\dot{m} \text{ is the mass flow rate of the refrigerant}) \quad (3.35)$$

The refrigerant leaving the evaporator is compressed to a relatively high pressure and temperature by the compressor. It is usually adequate to assume that there is no heat transfer to or from the compressor.

Conservation of mass and energy rate applied to a control volume enclosing the compressor then give:

$$\frac{\dot{W}}{\dot{m}} = h_2 - h_1 \quad \left(\frac{\dot{W}}{\dot{m}} \text{ is the work done per unit mass of refrigerant} \right) \quad (3.36)$$

Next, the refrigerant passes through the condenser, where the refrigerant condenses and there is heat transfer from the refrigerant to the cooler surroundings.

For a control volume enclosing the refrigerant side of the condenser, the rate of heat transfer from the refrigerant per unit mass of refrigerant is

$$\frac{\dot{Q}_{out}}{\dot{m}} = h_2 - h_3 \quad (3.37)$$

Finally, the refrigerant at state 3 enters the expansion valve and expands to the evaporator pressure. This process is usually modeled as a throttling process in which there is no heat transfer, i.e., for which

$$h_4 = h_3 \quad (3.38)$$

The temperatures of the refrigerant in the evaporator and condenser are the temperatures of the cold and warm regions, respectively, with which the system interacts thermally. This, in turn, determines the operating pressures in the evaporator and condenser. Consequently, the selection of a refrigerant is based partly on the suitability of its pressure-temperature relationship in the range of the particular application.

It is generally desirable to avoid excessively low pressures in the evaporator and excessively high pressures in the condenser. Other considerations in refrigerant selection include chemical stability, toxicity, corrosiveness, and cost. The type of compressor used also affects the choice of refrigerant.

Centrifugal compressors are best suited for low evaporator pressures and refrigerants with large specific volumes at low pressure. Reciprocating compressors perform better over large pressure ranges and are better able to handle low specific volume refrigerants.

Other considerations in refrigerant selection include chemical stability, toxicity, corrosiveness, and cost. A thermodynamic property diagram widely used in the refrigeration field is the pressure-enthalpy or p-h diagram.

3.13. Thermodynamic Modeling of Vapor Compression Cooling System

The cooling of a place with 200.000 kcal/h cooling load is studied with vapor compression system. Refrigerant R410A is preferred for this vapor compression system. Figure 3.15.shows the P-h diagram of R410A refrigerant.

T_6 is defined in equation 3.39

$$T_6 = \frac{3T_5 + T_{50}}{4} \quad (3.39)$$

T_5 = Condenser temperature and change with environment hourly in Adana

T_{50} =condensed chiller water temperature (accepted 5°C low then T_5)

In P-h diagram

$$P_4 = P_5 \quad (3.40)$$

$$P_2 = P_3 = P_4 + 0,1 \quad (3.41)$$

$$T_7 = T_8 \quad (3.42)$$

$$h_7 = h_6 \quad (3.43)$$

$$P_9 = P_1 = P_8 - 0,1 \quad (3.44)$$

$$T_7 = T_8 \quad (3.45)$$

The Carnot Efficiency is defined below using the condenser and evaporator temperatures;

$$\varepsilon_{c,c} = \frac{T_E}{T_C - T_E} \quad (3.46)$$

The compressor is open type compressor therefore we can write;

$$T_9 = T_1 \quad (3.47)$$

$$P_9 = P_1 \quad (3.48)$$

Because of isentropic expansion, it can be written;

$$s_3 = s_1 \quad (3.49)$$

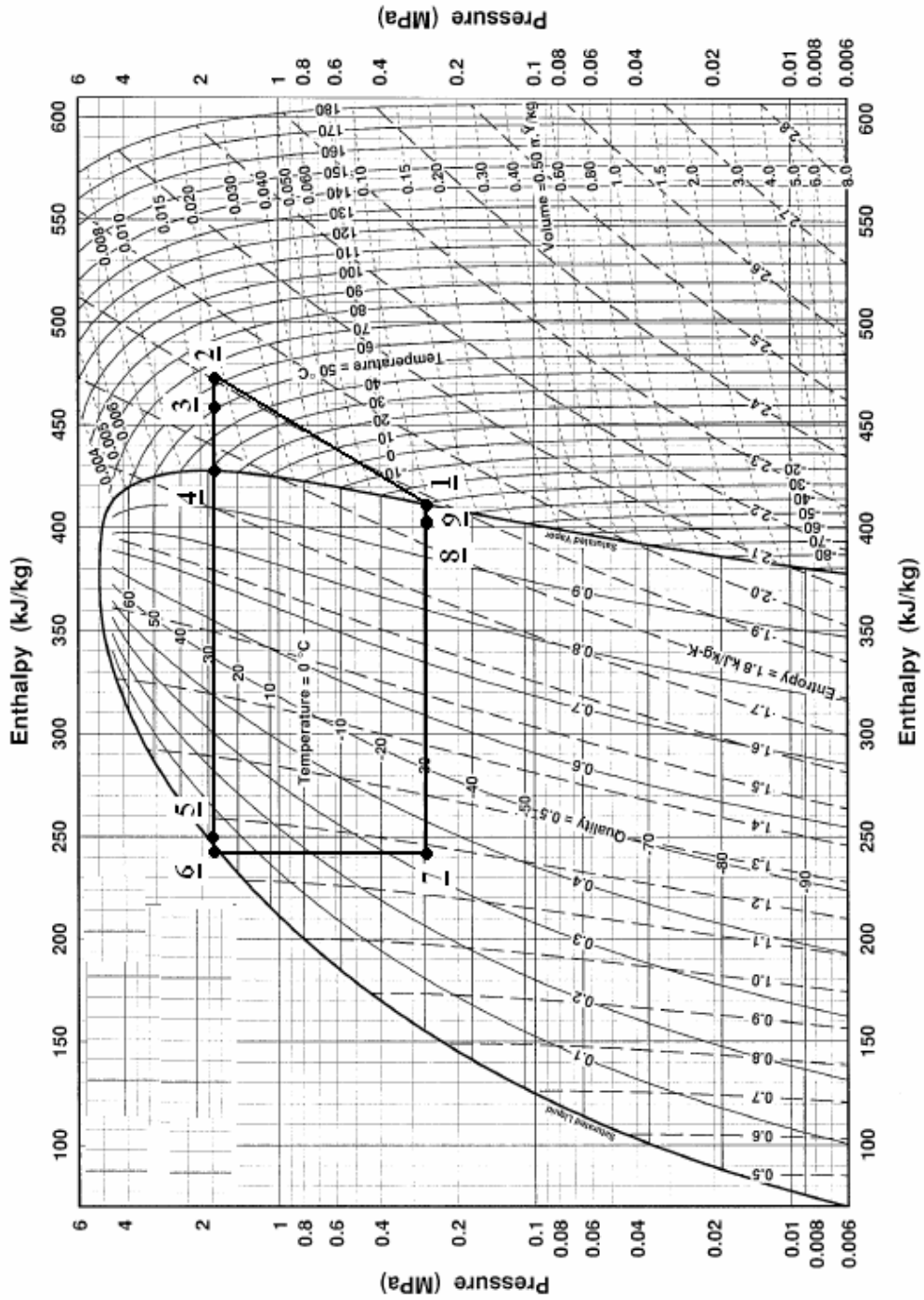


Figure 3.15. Pressure-Enthalpy diagram of refrigerant R410A

Pressure P_3 is known and consequently h_3 can be read in P-h diagram. The pressure ratio;

$$P^* = \frac{P_2}{P_1} \quad (3.50)$$

And the dead volume ratio;

$\varepsilon = 0,02$ are given η_v can be calculated from

$$\eta_v = 0,96 - \frac{1}{\left\{ 1 + \frac{2,1 - 40\varepsilon^{1,5}}{[\varepsilon(P^* - 1)]^2} \right\}^{0,5}} \quad (3.51)$$

η_{wl} is depends from V_{ge} value. However V_{ge} value is unknown yet.

Received heat in evaporator (Q_E) is determined with;

$$Q_E = M_R (h_9 - h_7) \quad (3.52)$$

Determined by M_R is the refrigerant flow rate; and defined that;

$$M_R = \frac{Q_E}{(h_9 - h_7)} \quad (3.53)$$

Volumetric flow rate of the refrigerant is than;

$$V_R = M_R v_1 \quad (3.54)$$

In equation 3.54. v_1 is specific volume at point 1.

The geometric is calculated approximate by as follows;

$$V_{ge} \approx \frac{V_R}{\eta_v - 0,15} \quad (3.55)$$

With these values, we can determine then;

$$\eta_{wl} = 0,095 \cdot V_{ge}^{-0,125} \cdot (P^* - 1)^{\frac{2}{3}} \quad (3.56)$$

With the determination of volumetric efficiency

$$\lambda = \eta_v - \eta_{wl} \quad (3.57)$$

We can determine than isentropic efficiency

$$\eta_i = \lambda \left\{ 1 - \varepsilon + (1,80\varepsilon^{1,125} + 0,005)(P^* - 1) \right\} \quad (3.58)$$

At Point 2 the enthalpy is calculated as follows;

$$h_2 = h_1 + \frac{h_3 - h_1}{\eta_i} \quad (3.59)$$

From the h_2 and h_3 values, the temperature T_2 and T_3 can be read from the diagram.

Coefficient of performance is defined for isentropic conditions and real conditions follow;

$$COP_{s,s} = \frac{h_9 - h_7}{h_3 - h_1} \quad (3.60)$$

$$COP_{s,i} = \frac{h_9 - h_7}{h_2 - h_1} \quad (3.61)$$

Isentropic power of compressor is given by;

$$W_{12} = M_R (h_2 - h_1) \quad (3.62)$$

Power of compressor shaft can be calculated by;

$$W_{KM} = \frac{W_{12}}{\eta_m} \quad (3.63)$$

Where η_m is mechanical efficiency. η_m can be determined by

$$\eta_m = 0,93 - \frac{0,75}{\sqrt{V_{ge} + 10}} \quad (3.64)$$

Power of transmission component (belt-pulley component efficiency $\eta_a = 0,9$) is given by

$$W_a = \frac{W_{KM}}{\eta_a} \quad (3.65)$$

The power of the electric motor can be calculated (can be accepted as $\eta_{emo} = 0,9$);

$$W_{emo} = \frac{W_a}{\eta_{emo}} \quad (3.66)$$

The coefficient of performance by the real cycle is then determined finally;

$$\varepsilon_s = \frac{Q_E}{W_{emo}} \quad (3.67)$$

3.14. Natural Gas Consumption of Absorption Cooling System

The coefficient of performance (COP) for cooling of the absorption system is defined as the heat load in the evaporator per unit of heat load in the generator and can be written as:

$$COP = \frac{Q_E}{Q_G} \quad (3.68)$$

Where;

COP= coefficient of the performance

Q_E = heat load in the evaporator (kcal/h)

Q_G = heat load in the generator (kcal/h)

In this equation; Q_E is constant every hour in a year and its value

$Q_E = 200.000$ kcal/h (234,8 kW/h) is assumed.

The COP is changed every hour in a year and its value is calculated with Artificial Neural Network (ANN) model. COP values calculated and shown in Table 3.4. These values give information for the year 2006 in Çukurova Region.

From the equation 3.68. energy need for the generator is determined ;

$$Q_G = \frac{Q_E}{COP} \quad (3.69)$$

Natural Gas consumption of absorption cooling depends on some parameters. These parameters are efficiency of natural gases, burning process, heating value of natural gas and heat load in the generator .These parameters effect directly natural gas consumption and shown in table 3.5. However Natural gas consumption can be defined below (Equation 3.70);

Table 3.5. Hourly natural gas consumption of absorption cooling system

date	hour	COP	LTV (kcal/m ³)	efficiency (η)	Q _E (kcal/h)	Q _G (kcal/h)	NGC (m ³)
04.01.2006	1	1,7244	8250	0,92	200000	115985	15,281
04.01.2006	2	1,7256	8250	0,92	200000	115902	15,270
04.01.2006	3	1,7265	8250	0,92	200000	115838	15,262
04.01.2006	4	1,7263	8250	0,92	200000	115854	15,264
04.01.2006	5	1,7261	8250	0,92	200000	115869	15,266
04.01.2006	6	1,7270	8250	0,92	200000	115807	15,258
04.01.2006	7	1,7256	8250	0,92	200000	115902	15,270
04.01.2006	8	1,7251	8250	0,92	200000	115934	15,275
04.01.2006	9	1,7194	8250	0,92	200000	116317	15,325
04.01.2006	10	1,7083	8250	0,92	200000	117075	15,425
04.01.2006	11	1,7050	8250	0,92	200000	117302	15,455
04.01.2006	12	1,7020	8250	0,92	200000	117512	15,482
04.01.2006	13	1,6988	8250	0,92	200000	117730	15,511
04.01.2006	14	1,6968	8250	0,92	200000	117871	15,530
04.01.2006	15	1,6980	8250	0,92	200000	117786	15,519
04.01.2006	16	1,7012	8250	0,92	200000	117566	15,490
04.01.2006	17	1,7035	8250	0,92	200000	117406	15,468
04.01.2006	18	1,7069	8250	0,92	200000	117174	15,438
04.01.2006	19	1,7069	8250	0,92	200000	117174	15,438
04.01.2006	20	1,7079	8250	0,92	200000	117100	15,428
04.01.2006	21	1,7104	8250	0,92	200000	116930	15,406
04.01.2006	22	1,7094	8250	0,92	200000	117002	15,415
04.01.2006	23	1,7087	8250	0,92	200000	117051	15,422
04.01.2006	24	1,7072	8250	0,92	200000	117149	15,435

$$NGC = \frac{Q_G}{\eta \times LTV} \quad (3.70)$$

Where;

NGC= natural gas consumption (m³/h)

Q_G = heat load in the generator (kcal/h)

η = burning efficiency of the natural gas

LTV=low heating value for natural gas (kcal/m³)

3.15. Electricity Consumption of Vapor Compression Cooling System

The cooling coefficient of performance (COP) for cooling of the absorption system is defined as the heat load in the evaporator per unit of heat load in the compressor and can be written as:

$$COP = \frac{Q_E}{Q_C} \quad (3.71)$$

Where;

COP= coefficient of the performance

Q_E = heat load in the evaporator (kcal/h)

Q_C = heat load in the compressor kcal/h)

In this equation; Q_E is constant every hour in a year and its value

$Q_E = 200.000$ kcal/h (234,8 kW/h) is assumed..

The COP is changed every hour in a year and its value calculated in past chapters. COP values are shown in Figure 3.16. These values give information for the year 2006 in Çukurova Region. From equation 3.71. Q_C can be determined as follows;

$$Q_C = \frac{Q_E}{COP} \quad (3.72)$$

Electricity consumption of vapor compression cooling system depends on some parameters.

Heat consumption of the compressor is calculated from;

$$Q_C = EC \times \eta \times LTV \quad (3.73)$$

Where;

EC= electricity consumption (kW/h)

Q_C = heat load in the compressor (kcal/h)

η = efficiency of the electricity

LTV=lower heating value for electricity generation (kcal/kW)

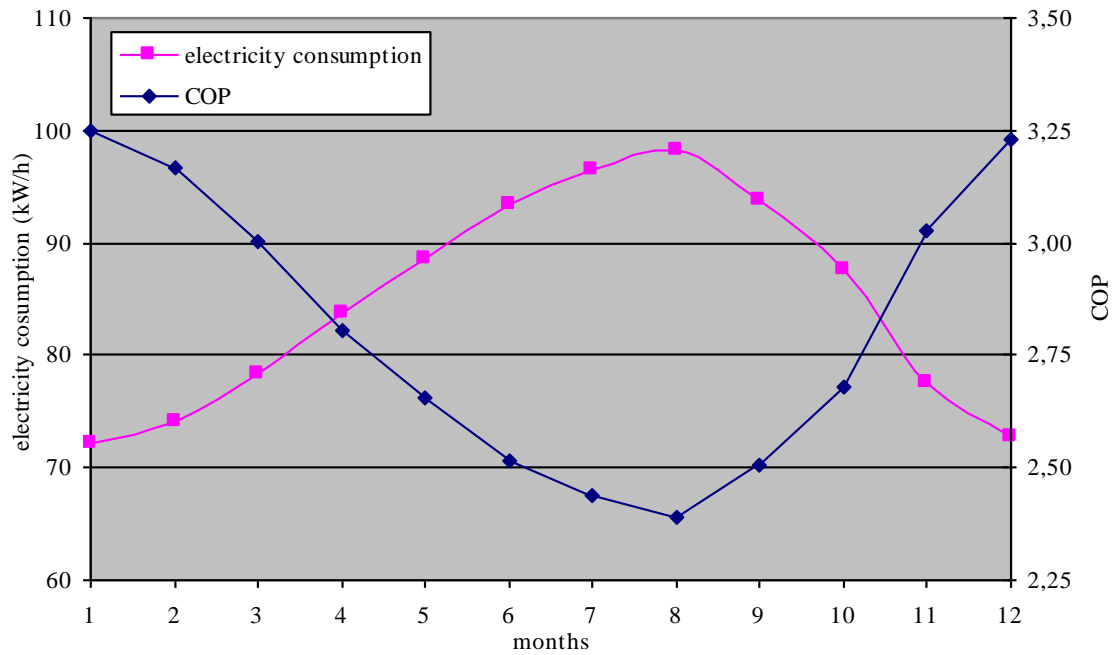


Figure 3.16. Distribution COP-electricity consumption for the year 2006

Table 3.6. Monthly electricity consumption of vapor compression cooling system

month	COP	LTV (kcal/kW)	efficiency (η)	Q_E (kcal/h)	Q_C (kcal/h)	EC (kW/h) hourly	Total consumption (kW/month)
January	3,2512	860	0,99	200000	61516	72,253	53756,24
February	3,1685	860	0,99	200000	63122	74,139	49821,32
march	3,0008	860	0,99	200000	66650	78,283	58242,33
April	2,8072	860	0,99	200000	71244	83,679	60248,78
may	2,6543	860	0,99	200000	75349	88,500	65844,20
June	2,5141	860	0,99	200000	79552	93,437	67274,71
July	2,4359	860	0,99	200000	82105	96,436	71748,05
August	2,3915	860	0,99	200000	83628	98,224	73078,60
September	2,5070	860	0,99	200000	79775	93,699	67463,12
October	2,6819	860	0,99	200000	74574	87,590	65166,73
November	3,0265	860	0,99	200000	66083	77,617	55884,16
December	3,2305	860	0,99	200000	61909	72,715	54099,91

3.16. Economic Analysis of a Project

The aim of the economic analysis of this project is to maintain a better allocation of sources, which leads to enhanced incomes for investment. For a directly productive project, for which the output is sold in a competitive environment, the selected projects meet a minimum standard for resource generation and the choices should have to be made to eliminate the projects that do not meet the standards.

There are four basic steps in analyzing the economic feasibility of a project:

1. Identifying the economic costs and benefits
2. Quantifying the costs and benefits
3. Determining the values of the costs and benefits
4. Comparing the benefits with the costs

3.16.1. Identification and Quantification of Benefits

For directly productive projects, the main benefits will be the net income gained from the production that is sold. While forecasting this income, it is first necessary to determine whether the project is incremental or not. If the project size is small with respect to the market size, it is usually the case that the project is fully incremental. Otherwise, the project can cause price effects where non-incremental output displaces sales from higher-cost manufacturer (Park 2001, Sepulveda et al. 1984, Castillo 1998).

For indirectly productive projects, the needs for services depend on the underlying factors such as the rate of electricity consumption. The key feature for these projects is to make an investment to meet the demand. In much of the indirectly productive projects, the project benefits can be quantified as time and cost savings, improved health, and so on (Park 2001, Sepulveda et al. 1984, Castillo 1998).

3.16.2. Identification and Quantification of Costs

Several types of costs need to be included in the economic analysis of a project. While quantifying these costs, the project that are going to be quantified are found by calculating the difference in costs between the without and with project situations, that is the extra use of resources necessary to achieve the corresponding benefits. The types of costs that can be incurred during a project are explained separately below.

3.16.3. System Costs

If a project is a part of a larger project and incremental, it cannot be applied unless matching investments at the whole system has been made. For example, when increasing the power generation capacity, it is also necessary to make some investments on the existing transmission and distribution systems. The project should include the costs of the whole system required to achieve the benefits. If the total system of projects is viable, then the project is also viable.

3.16.4. Time Value of Money

Time value of the money suggests that money available at the present time worth more than the same amount in the future, due to its potential to earn money. Provided money can earn money, which yields the result that the same amount of money worth more the sooner it is received.

To understand the time value of money clearly it is first necessary to understand the interest and the interest rate concepts. The return derived from an investment is interest, and the fraction by which the return of the investment calculated is called the interest. To find the interest of a project, interest rate is applied to the present worth of the investment.

When this interest is added to the present worth, the future worth of the investment can be found. Future worth can also be found by adding 1 to the interest rate and directly multiplying that value with the present worth of the investment. The formula to find the future worth of an investment is given below.

$$FV = PV \times (1 + i) \quad (3.74)$$

Where,

FV = Future value of the investment

PV = Present Value of the investment

i = Interest rate

3.16.5. Simple Payback Period Method

Payback considers the initial investment costs and the resulting annual cash flow. The payback time (period) is the length of time needed before an investment makes enough to recoup the initial investment. But the payback method doesn't account for savings after the initial investment is paid back from the profits (cash flow) generated by the investment (project). This method is a "first cut" analysis to evaluate the viability of investment.

Payback period is calculated using the following equation if the annual savings are equal:

$$\text{Payback Period (in years)} = \frac{\text{Initial Investment}}{\text{Annual Savings (Cash Flow)}} \quad (3.75)$$

Where;

Initial Investment – Initial investment for a project

Annual Savings (Cash Flow) – Annual savings derived from the investment.

Consider an example of evaluating the purchase of pollution prevention equipment for a cost of \$8,000, but provide a net annual operational saving of \$3,500. When the net annual savings is divided into the initial investment, the sample payback period is calculated as follows:

$$\text{Payback Period (in years)} = \frac{\text{Initial Investment}}{\text{Annual Savings (Cash Flow)}} = \frac{8000}{3500} \approx 2.3 \text{ (years)}$$

However, there are significant costs such as depreciation and taxes, which will cause cash flows differs from year to year, the payback period is determined when the accrued cash savings equal the initial investment.

For simple payback period, other significant costs such as depreciation and taxes are ignored in the calculation.

3.16.6. Net Present Value Method

NPV is an indicator of how much value an investment or project adds to the firm. With a particular project, if R_t is a positive value, the project is in the status of discounted cash inflow in the time of t . If R_t is a negative value, the project is in the status of discounted cash outflow in the time of t .

Appropriately risked projects with a positive NPV could be accepted. This does not necessarily mean that they should be undertaken since NPV at the cost of capital may not account for [opportunity cost](#), i.e. comparison with other available investments. In financial theory, if there is a choice between two mutually exclusive alternatives, the one yielding the higher NPV should be selected.

Each cash inflow/outflow is [discounted](#) back to its present value (PV). Then they are summed. Therefore NPV is the sum of all terms;

$$\frac{R_t}{(1+i)^t} \quad (3.76)$$

Where;

t = the time of the cash flow

i = the [discount rate](#) (the [rate of return](#) that could be earned on an investment in the financial markets with similar risk.)

R_t = the net cash flow (the amount of cash, inflow minus outflow) at time t (for educational purposes, R_0 is commonly placed to the left of the sum to emphasize its role as (minus the) investment).

$$NPV = \sum_{m=m+1}^t \frac{F_n}{(1+i)^n} - \sum_{n=0}^m \frac{M_n}{(1+i)^n} \quad (3.77)$$

Where;

NPV= net present value

M_n = investment in year n

i = the market discount rate

F_n = benefit in year n

m= end of investment year

t-m= economical life of project

The following sums up the NPVs in various situations in table 3.7..

Table 3.7. Various situations of NPV

IF	IT MEANS	THEN
NPV > 0	the investment would add value to the firm	the project may be accepted
NPV < 0	the investment would subtract value from the firm	the project should be rejected
NPV = 0	the investment would neither gain nor lose value for the firm	We should be indifferent in the decision whether to accept or reject the project.

However, NPV = 0 does not mean that a project is only expected to break even, in the sense of undiscounted profit or loss (earnings). It will show net total positive cash flow and earnings over its life.

3.16.7. Internal Rate of Return Method

The internal rate of return (IRR) is a [capital budgeting](#) metric used by firms to decide whether they should make [investments](#). It is also called discounted cash flow rate of return (DCFROR) or rate of return (ROR). It is an indicator of the efficiency or quality of an investment, as opposed to [net present value](#) (NPV), which indicates value or magnitude.

The IRR is the annualized effective compounded return rate which can be earned on the invested capital, i.e., the [yield](#) on the investment. Put another way, the internal rate of return for an investment is the discount rate that makes the net present value of the investment's cash flow stream equal to zero.

$$NPV = \sum_{m=m+1}^t \frac{F_n}{(1+i)^n} - \sum_{n=0}^m \frac{M_n}{(1+i)^n} = 0 \quad (3.78)$$

The Internal rate of return (IRR) is the rate of return produced by each money for the amount of time that dollar is in the investment. Given a collection of pairs (time, [cash flow](#)) involved in a project, the internal rate of return follows from the [net present value](#) as a function of the [rate of return](#).

$$IRR = \sum_{m=m+1}^t \frac{F_n}{(1+r)^n} = \sum_{n=0}^m \frac{M_n}{(1+r)^n} \quad (3.79)$$

Where;

IRR= Internal rate return

M_n = investment in year n

r= Internal rate

F_n = benefit in year n

m= end of investment year

t-m= economical life of project

4. RESULTS AND DISCUSSION

In this study, the performance and economical analysis of the absorption and vapor compression cooling systems designed under the conditions of Çukurova Region (in Adana) is analyzed using the hourly outdoor temperature, which were measured by DMI (Turkish State Meteorological Service) for the year 2006. Furthermore the economical life and performance of the systems are analyzed for a year hour by hour.

During the study, two different cooling systems (absorption cooling with natural gas and vapor compression cooling systems) are analyzed and compared individually.

The first analyzed system is absorption cooling which is calculated using the equations which are given above (Equations 3.1. to 3.34.) and the values given random days and hours in Table 4.1.

Table 4.1. shows results of absorption cooling calculations with ANN for random days and hours. In additionally Figure 4.1. shows and compare temperature-COP values yearly for all hours. In winter months; the outdoor temperature decrease and therefore the COP values increase and these changes can be shown in Figure 4.1. easily. In summer months; the outdoor temperature increase depending on this the COP values decrease.

In this study the minimum temperature is recorded as $-2,8\text{ }^{\circ}\text{C}$ in 28/12/2006 at 07:00, and COP of absorption cooling system is calculated as 1,7393. This value is the maximum calculated COP in this project. The maximum temperature is recorded as $38,8\text{ }^{\circ}\text{C}$ in 20/08/2006 at 14:00 and 15:00, depending on this COP of absorption cooling system is calculated 1,520. This value is the minimum calculated COP in this project. Average COP found in this project 1,6812.

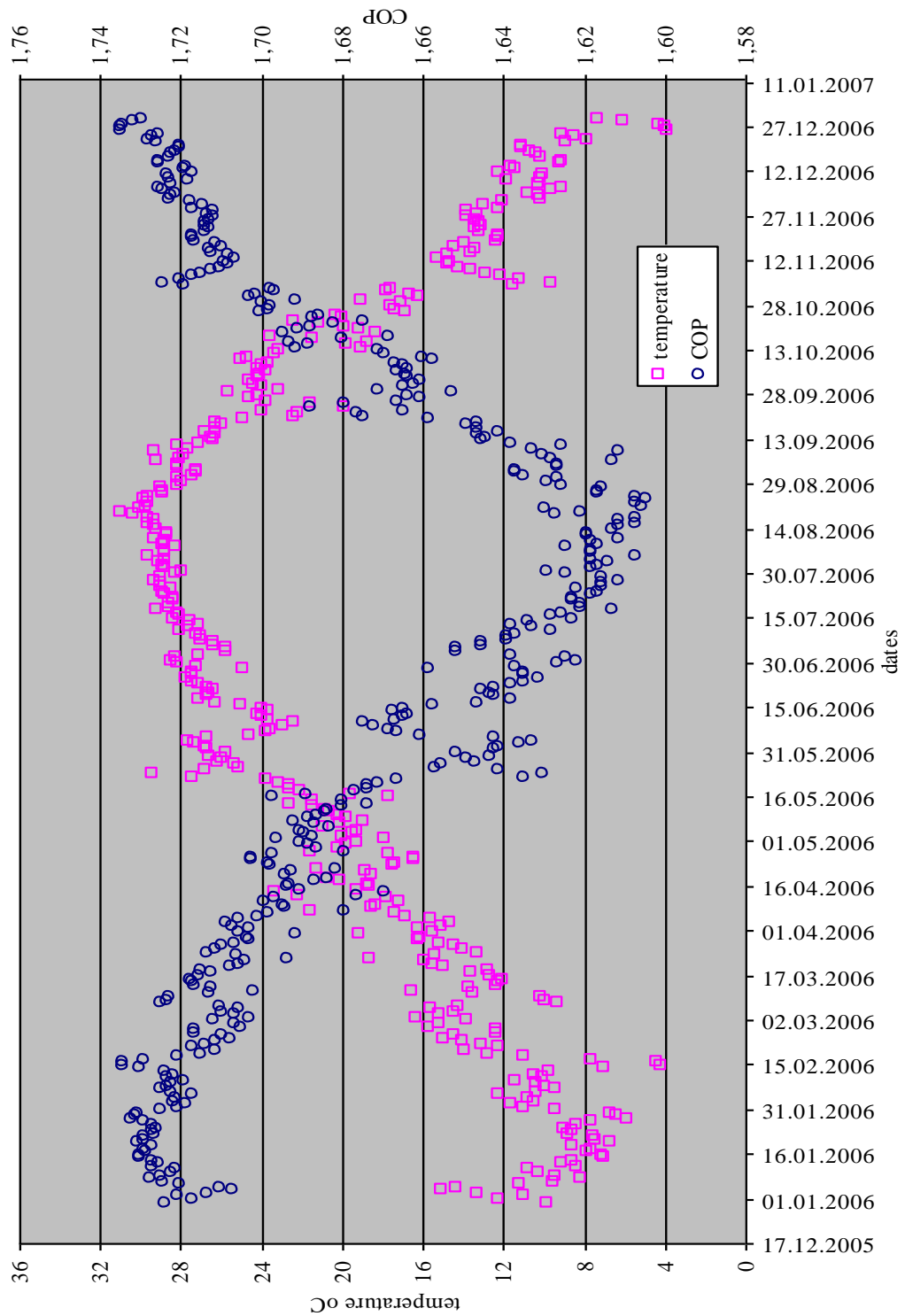


Figure 4.1. Distribution of COP and temperature of absorption cooling system in the year 2006

Table 4.1. The values and results used in absorption cooling system calculated with ANN

date	hour	evaporator temperature T_E ($^{\circ}\text{C}$)	absorber temperature T_A ($^{\circ}\text{C}$)	condenser temperature T_C ($^{\circ}\text{C}$)	low generator temperature T_{Gl} ($^{\circ}\text{C}$)	high generator temperature T_{Gh} ($^{\circ}\text{C}$)	COP
01.01.2006	1	7	15,9	25,9	114	180	1,73
01.01.2006	2	7	15,9	25,9	114	180	1,73
04.02.2006	17	7	26	36	114	180	1,70
04.02.2006	18	7	24,3	34,3	114	180	1,71
14.03.2006	14	7	29,6	39,6	114	180	1,69
14.03.2006	15	7	28,9	38,9	114	180	1,69
14.03.2006	16	7	28	38	114	180	1,70
14.03.2006	21	7	21,1	31,1	114	180	1,72
14.03.2006	22	7	20,9	30,9	114	180	1,72
10.04.2006	5	7	25,5	35,5	114	180	1,71
10.04.2006	6	7	25,1	35,1	114	180	1,71
15.05.2006	14	7	40	40	114	180	1,63
15.05.2006	15	7	38,9	48,9	114	180	1,62
23.06.2006	1	7	34,7	44,7	114	180	1,66
23.06.2006	2	7	34,8	44,8	114	180	1,66
25.07.2006	6	7	35,6	45,6	114	180	1,65
25.07.2006	7	7	36,8	46,8	114	180	1,64
04.09.2006	19	7	37,8	47,8	114	180	1,63
04.09.2006	20	7	37,2	47,2	114	180	1,64
11.10.2006	23	7	32,4	42,4	114	180	1,67
11.10.2006	24	7	31,9	41,9	114	180	1,68
02.12.2006	5	7	15,7	25,7	114	180	1,73
02.12.2006	6	7	16	26	114	180	1,73

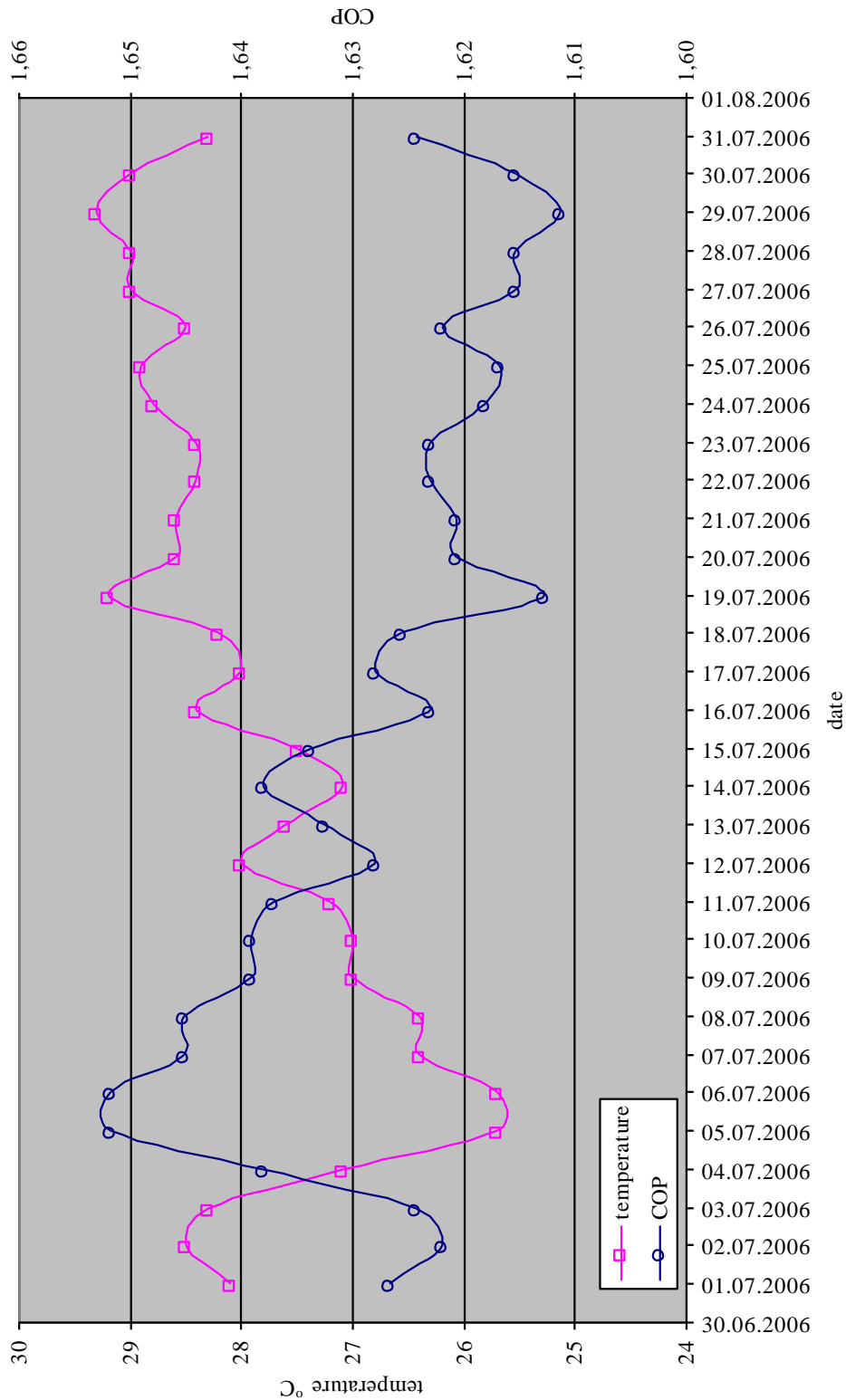


Figure 4.2. Distribution of COP and temperature of absorption cooling system in July-2006

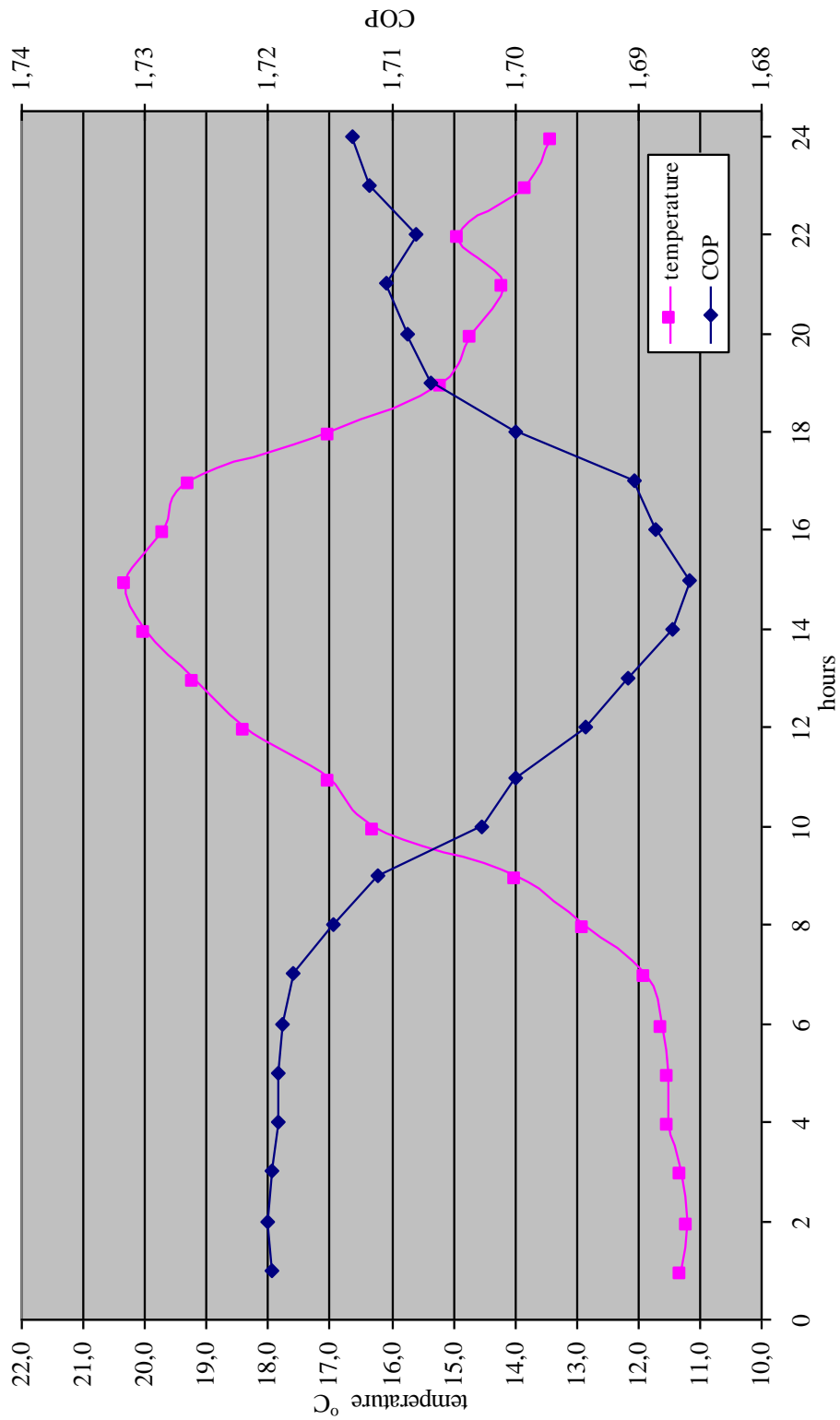


Figure 4.3. Distribution of COP and temperature of absorption cooling System in 21 March 2006

A randomly chosen day COP-temperature distribution is shown in Figure 4.3.

The energy consumption is very necessary for the economical analysis. Therefore natural gas consumption for absorption cooling system is calculated using the equations which are given (in Equation 3.64. to 3.66.) and coefficient of performance (COP) and natural gas consumption are shown in Figure 4.4.

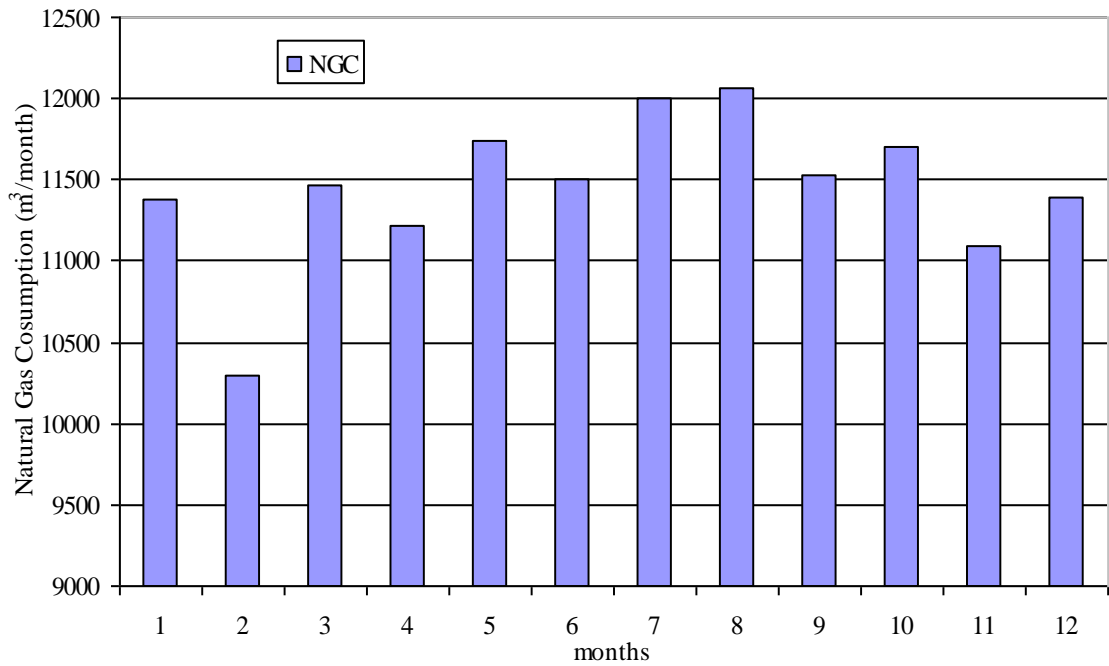


Figure.4.4. Distribution of COP and NGC monthly year of 2006

The maximum and minimum natural gas consumptions are shown monthly in Figure 4.5. The maximum natural gas consumption value is 12068 m^3 in August; however the minimum natural gas consumption value is 10300 m^3 in February. Total natural gas consumption is 137384 m^3 in 2006.

The second analyzed system is vapor compression cooling and this system is calculated using the equations given above (Equations 3.35. to 3.63.).The results for all months in 2006 are shown in Figure 4.6.

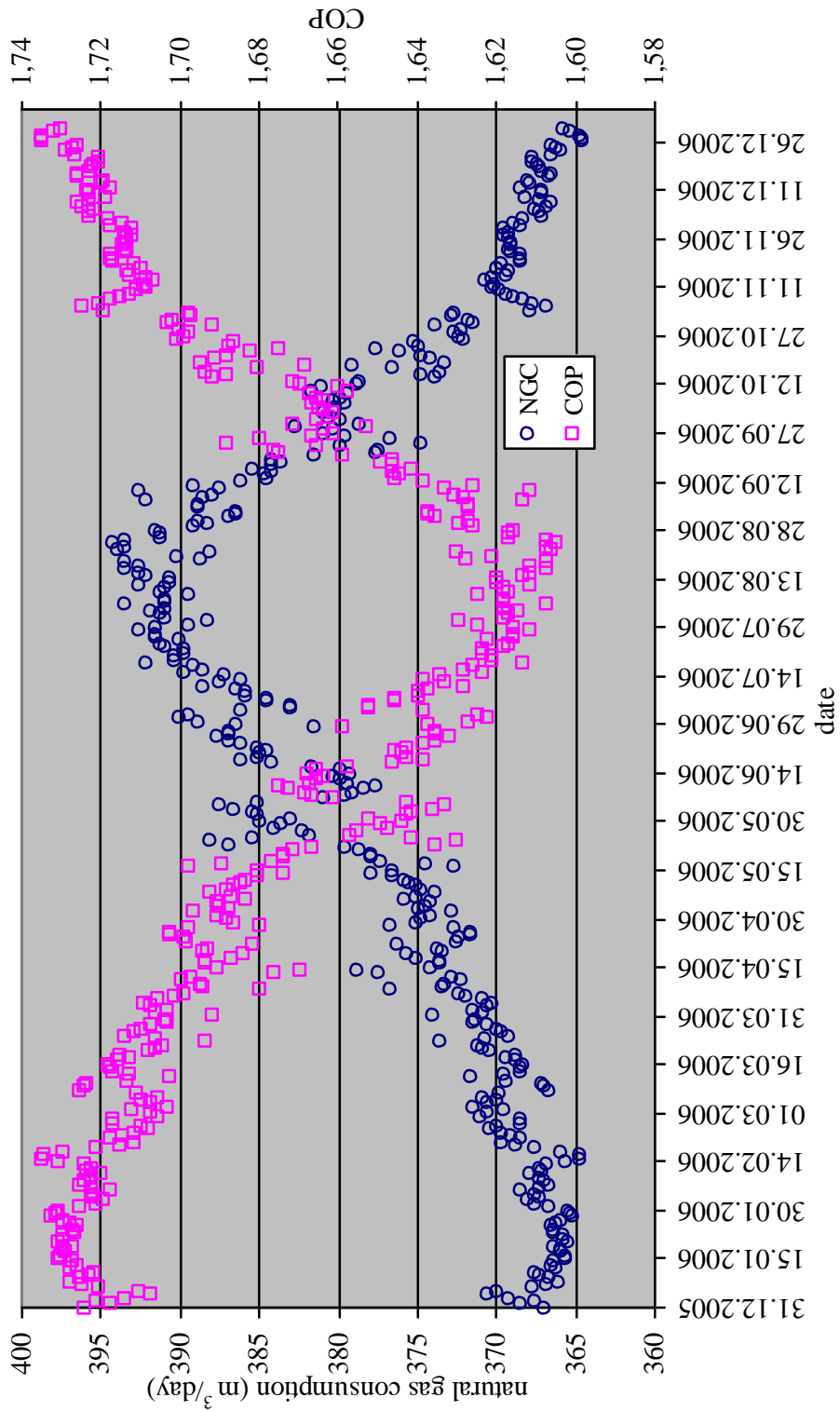


Figure 4.5. Distribution of COP and NGC daily for the year 2006

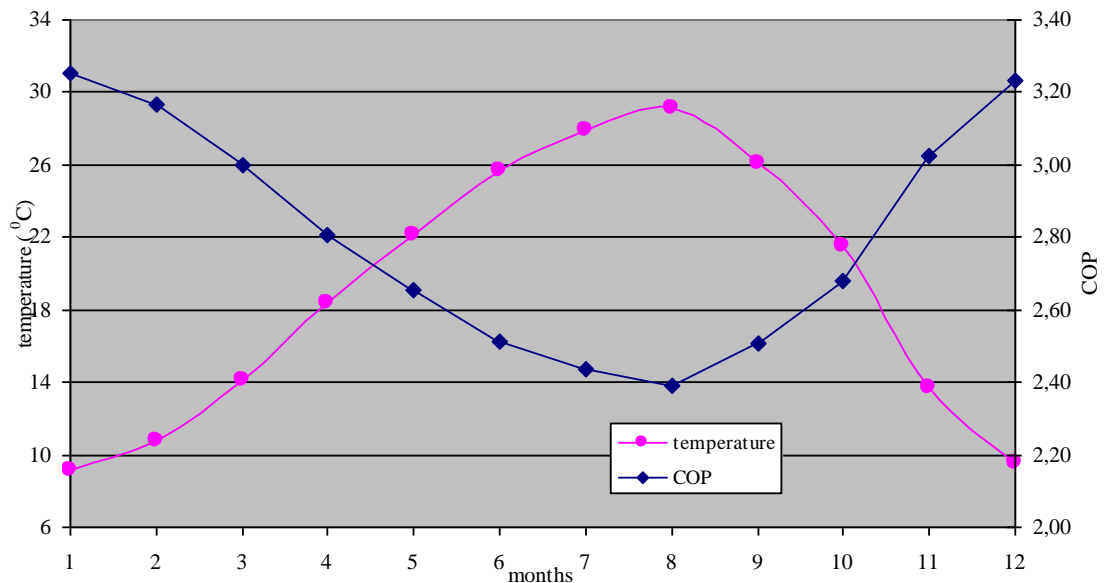


Figure 4.6. Distribution of COP and temperature for vapor compression cooling system

The electricity consumption is very necessary to compare the advantage of the absorption cooling system in this project. Therefore electricity consumption for absorption cooling system is calculated using the equations which are given above (in Equation 3.67. to 3.69).

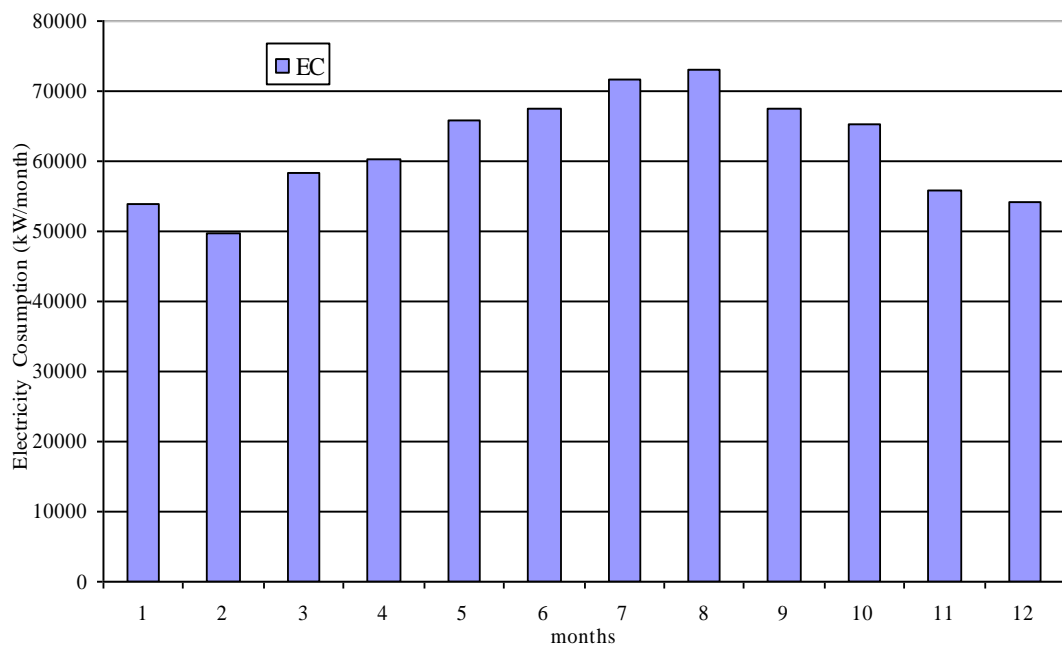


Figure.4.7. Distribution of COP and EC monthly for the year 2006

The maximum and minimum electricity consumptions are shown monthly in Figure 4.7. The maximum electricity consumption value is 73126 kW in August; however the minimum electricity consumption value is 49821 kW in February. Total electricity consumption is 742637 kW in 2006.

The main purpose of this project was to compare two cooling systems economically. Therefore the prices of natural gas and electricity are important consequently. The companies of BOTAŞ (Petroleum Pipeline Corporation of Turkey) and TEDAŞ (Turkish Electricity Distribution Corporation) specify in an arrangement to set these prices. Electricity and natural gas price information's are shown in Appendix A1.

Absorption cooling system requirements and operation costs are given the Table 4.2. Total consumption of natural gas is 137384 m³ depending on this the total operation cost in 2006 is 42328 €.

Vapor compression system requirements and operation costs are given the Table 4.3. Total consumption of electricity is 742637 kW and depending on this the total operation cost in 2006 is 85775 €.

Table 4.2. Monthly operation costs of absorption cooling system in 2006

months	COP	unit price (€/m ³)	unit price (TL/m ³)	need of cooling load (kcal/h)	required of cooling load (kcal/h)	natural gas consumption (m ³)	total operation cost(€)	total operation cost(TL)
January	1,72	0,3081	0,65	200000	116022,89	11373,37	3504,14	7432,50
February	1,72	0,3081	0,65	200000	116323,48	10299,56	3173,29	6730,76
March	1,71	0,3081	0,65	200000	117023,08	11471,84	3534,47	7496,85
April	1,69	0,3081	0,65	200000	118236,05	11217,79	3456,20	7330,82
May	1,67	0,3081	0,65	200000	119710,75	11738,97	3616,78	7671,41
June	1,65	0,3081	0,65	200000	121215,01	11501,41	3543,58	7516,17
July	1,63	0,3081	0,65	200000	122364,44	11996,38	3696,09	7839,64
August	1,62	0,3081	0,65	200000	123093,40	12068,15	3718,20	7886,54
September	1,65	0,3081	0,65	200000	121436,16	11524,11	3550,58	7531,00
October	1,67	0,3081	0,65	200000	119413,63	11708,55	3607,40	7651,54
November	1,71	0,3081	0,65	200000	116964,28	11096,47	3418,82	7251,54
December	1,72	0,3081	0,65	200000	116158,46	11387,01	3508,34	7441,41
						TOTAL	42.327,89 €	89.780,18 TL

Table 4.3. Monthly operation costs of vapor compression system in 2006

months	COP	unit price (€/kWh)	unit price (TL/kWh)	need of cooling load (kcal/h)	required of cooling load (kcal/h)	electricity consumption (kW)	total operation cost(€)	Total operation (TL)
January	3,25	0,1155	0,2451	200000	61516,21	53756,23	6208,84	13175,65
February	3,17	0,1155	0,2451	200000	63121,83	49820,94	5754,32	12211,11
March	3,00	0,1155	0,2451	200000	66649,90	58256,99	6728,68	14278,79
April	2,81	0,1155	0,2451	200000	71244,18	60189,75	6951,92	14752,51
May	2,65	0,1155	0,2451	200000	75349,13	65951,31	7617,38	16164,67
June	2,51	0,1155	0,2451	200000	79552,34	67383,74	7782,82	16515,76
July	2,44	0,1155	0,2451	200000	82105,23	71627,44	8272,97	17555,89
August	2,39	0,1155	0,2451	200000	83627,85	73125,93	8446,04	17923,16
September	2,51	0,1155	0,2451	200000	79775,14	67383,74	7782,82	16515,76
October	2,68	0,1155	0,2451	200000	74573,86	65213,05	7532,11	15983,72
November	3,03	0,1155	0,2451	200000	66083,02	55819,54	6447,16	13681,37
December	3,23	0,1155	0,2451	200000	61909,49	54108,66	6249,55	13262,03
TOTAL							85.774,6 €	182.020,40 TL

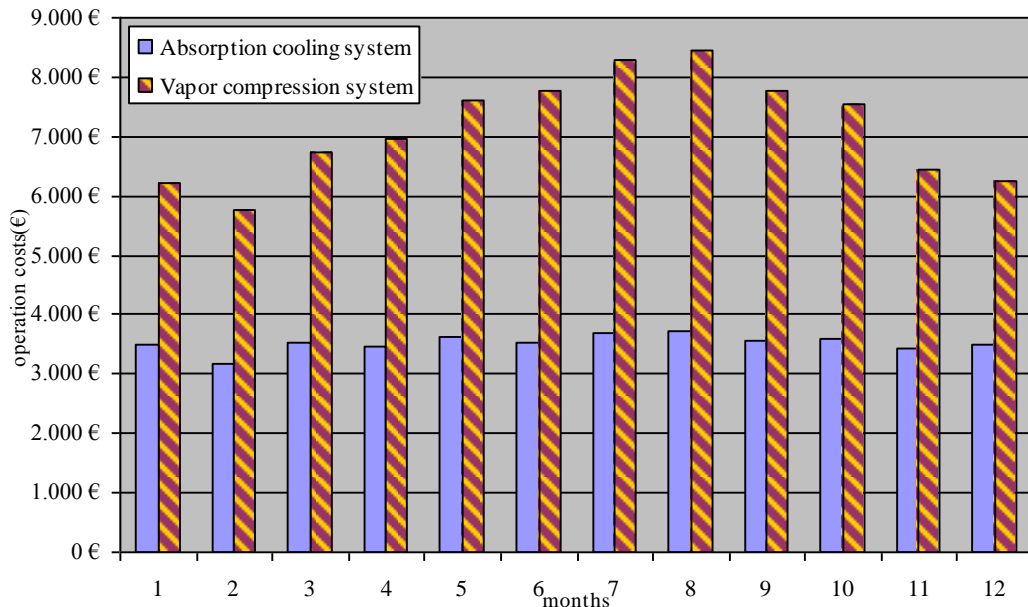


Figure 4.8. Comparison of operation costs for absorption and vapor compression cooling systems

The vapor compression cooling system COP is higher than that of the absorption cooling system. However the operation cost is much higher than the other system. The main reason is electricity-natural gas price difference.

Simple payback, net present value and internal rate of return methods are commonly used for economical analysis of two or more systems. Investment costs, savings, discount rate and life of investment required for the calculations. Required parameters are given Table 4.4.

Although, investment costs, economical life of investments, repair and maintenance costs, salvage cost etc. values are given by Alarko-Carrier Company of Turkey. Alarko-Carrier suggest to 30 RB 232 model for vapor compression cooling system and 16DN015 model for absorption cooling system. These models technical and economical information's are shown in Appendix A2 and A3.

Table 5.5. shows that the economical method results for absorption and vapor compression cooling systems. The calculation results show that the absorption cooling system is more advantageous and economic than the vapor compression cooling system.

Table 4.4. Costs and parameters for economical analysis

	Absorption cooling system	Vapor compression system
Investment cost (€)	84.700 €	31.900 €
Annular operation cost (€)	42.327 €	85.774 €
Repair and maintenance cost (triennial) (€)	2.000 €	3.000 €
Salvage value (€)	15.000 €	5.000 €
Annular saving (€)	57.672 €	14.225 €
Economical life (n)	15	15
discount rate	10%	10%

Table 4.5. Economical analysis of absorption and vapor compression cooling systems

Method/Cooling System	Absorption Cooling System	Vapor Compression Cooling System
Simple payback (year)	1,5	2,2
Expense (€)	91.399,27 €	43.643,74 €
Benefit (€)	442.249,53 €	109.396,48 €
Benefit (€) / Expense (€) ratio	4,84	2,51
Net Present Value	350.850,27 €	65.752,74 €
Internal Rate of Return (%)	53,66	25,49

5.CONCLUSIONS

In this study, implementation of an absorption cooling system into a place in Çukurova Region, which uses natural gases as the primary energy source has been examined. During the study, two different cooling machines (absorption cooling and vapor compression cooling) with same capacities have been considered. The conventional cooling systems are not economical in today conditions.

This study aimed to identify the role of cooling systems to reduce the energy costs by using the absorption cooling systems with natural gas. So, the calculations are usually based on the comparison of the natural gas cost of the absorption cooling systems and the electricity costs of the vapor compression cooling systems. The results are determined for two pricing options, kWh pricing and m³ pricing.

COP values of absorption cooling system given in Figure 4.1. and natural gas consumption values are given in Figure 4.5. , Figure 4.6. and Table 4.2. These figures and tables show that the energy consumptions depend on COP. General COP values of absorption cooling system are lower than the other cooling systems, however the natural gas prices are lower than the other energy types. Price of Natural gas is set as 0,3081 €/m³ by BOTAŞ.

COP values of vapor compression cooling system are given in Figure 4.6. and electricity consumption values are given in figure 4.7. and table 4.3. Vapor compression systems are more effective than the absorption cooling systems. However the energy prices are too high in Turkey. Price of the electricity is set of 0,1155 €/kWh by TEDAS.

Table 4.4. shows that the economical conditions of absorption and vapor compression cooling systems clearly. Investment costs of absorption cooling system is 84.700€ and higher than the vapor compression cooling system. Investment costs of vapor compression cooling system is 31.900 €.

At first appearance, the vapor compression cooling system is more advantageous due to COP values and investment costs. However the operation costs of these two systems are very different. Operation costs by order of absorption and vapor compression cooling systems are 42.328 € and 85.775 € per year.

These investment and operation costs are calculated together with economical analysis methods and results are shown in Table 4.5. All methods and calculations show that the absorption cooling system is more advantageous and effective due to the low natural gas prices.

In the future studies, the use of alternative energy sources such as solar energy and geothermal energy should be investigated in detail. The design of such systems, feasibility, thermodynamic analysis and possible advantages and disadvantages during operation of systems should be discussed.

REFERENCES

- Absorption Chillers,(1998). Southern California Gas Company New Buildings Institute Advanced Design Guideline Series, Report BNL 32223.
- AKKUS, S., ÇAGLA, H.,(2007). Petrol and Natural Gas Distribution Lines in Turkey And Cartography Studies, Strategic Integration of Surveying Services FIG Working Week 2007 Hong Kong SAR, pp. 11-34.
- Alarko-Carrier, (2009).Alarko-Carrier products, <http://www.alarko-carrier.com.tr/#>.
- ASHRAE, (2001). Fundamentals Handbook (SI), Psychometrics, Vol.6, pp. 1-12.
- ASHRAE, (1997). Fundamentals Handbook (SI), ASHRAE TC 3.1. Refrigerants and Brines, Vol.17-64 to 17-68.
- BOTAŞ, (2009). BOTAŞ web Site, <http://www.botas.gov.tr>.
- CASTELLS, F., BRUNO, J.C.,(2000). Optimization of energy plants including water/lithium bromide absorption chillers, International Journal of Energy Research, vol.24, pp.695-717.
- CASTILLO, C.P., (1998). Economic Analysis of Social Investment Fund Projects, World Bank, Washington D.C., pp. 1-2.
- CHUA, H.T., TOH, H.K., (2000).Thermodynamic modeling of an ammonia–water absorption chiller, International Journal of Refrigeration vol.25, pp. 896–906.
- EICKER, U., (2003).Solar Technologies for Buildings, John Wiley&Sons, West Sussex, pp. 177-182.
- FLORIDES, G.A., KALOGIROU, S.A., TASSOU S.A., WROBEL, L.C., (2003).Design and Construction of a LiBr-Water Absorption Machine, Energy Conversion and Management Journal, Vol. 44, No. 15, pp. 2483-2508.
- GROSSMAN, G., (2002).Solar-Powered Systems for Cooling, Dehumidification and Air-Conditioning, Solar Energy Journal, Vol. 72, No. 1, pp. 53-62.
- HEROLD,K.E., RODERMACHER, R., KLEIN, S.A.,(1996).Absorption Chillers and Heat Pumps, CRC Press, Florida, pp. 235-242.
- HONDEMAN, H., (2000).Electrical Compression versus Absorption Cooling-A Comparison, Heat Pump Center Newsletter, Vol. 18, No. 4, pp. 23-25.

- İGDAŞ, (2009). İGDAŞ web Site, <http://www.igdas.com.tr>.
- İMAN, H., BAHCE, İ.G.,(2001).Doğalgazlı Soğutma , VII. ULUSAL TESİSAT MÜHENDİSLİĞİ KONGRESİ, pp. 65-82.
- LAZZARIN, R., LONGO,G.A., GASPARALLA, A.,(1996).Ammonia-Water Absorption Machines for Refrigeration: Theoretical and Real Performances, International Journal of Refrigeration, Vol. 19, No. 4, p. 247.
- MANOHAR, H.J., SARAVANAN, R., (2005). Modeling of steam fired double effect vapor absorption chiller using neural network, Energy Conversion and Management vol. 47, pp. 2202–2210.
- MAIDEMENT, G.G., TOZER, R.M.,(2002).Combined Cooling Heat and Power in Supermarkets, Applied Thermal Engineering Journal, Vol. 22, pp. 653-665.
- ODABASI, H, (2001).Absorption Cooling Systems and Cogeneration, Installment Journal (In Turkish), No. 69, pp. 124-130.
- PARK, C.S, (2001). Contemporary Engineering Economics, Prentice Hall, New Jersey, pp. 62-80.
- SEPULVEDA J.A., SOUDER W.E., GOTTFRIED B.E., (1984).Schaum’s Outline of Engineering Economics, McGraw Hill, New York, pp. 1-15.
- SODHA, M.S., MATHUR, S.S., MALIK, M.A.S., (1983). Reviews of Renewable Energy Resources, Wiley Eastern Limited, New Delhi, pp. 28-32.
- SRIKHIRIN, P., APHORNROTANA, S., CHUNGPAIBULPATANA, S.,(2001). A review of Absorption Refrigeration Technologies, Renewable and Sustainable Energy Reviews, Vol.5, No. 4, pp. 343-372.
- SHUN-FU, L. and SHERIF, S. A.,(2001).Thermodynamic analysis of a lithium bromide/water absorption system for cooling and heating applications, Int. J. Energy Res. 2001; 25:1019 1031 (DOI: 10.1002/er.738).
- ŞENCAN, A., YAKUT, K.A., KALOGIROU, S.A.,(2004).Thermodynamic analysis of absorption systems using artificial neural network, Science Direct, Renewable Energy 31, pp. 29–43.

- ŞENCAN, A.,(2004). A different approach for the analysis of a double-effect absorption refrigeration system operating with LiBr + LiNO₃ + LiI + LiCl / H₂O, J. Fac. Eng. Arch. Gazi Univ., vol. 21, No 3, 467-472.
- TOZER, R.M., JAMES, R.W.,(1997).Fundamental Thermodynamics of Ideal Absorption Cycles, International Journal of Refrigeration, Vol. 20, No. 2, pp. 120-135.
- TRNSYS, (2009).TRNSYS HVAC simulation web Site, <http://www.trnsys.com>
- WANG, S.K., LAVAN, Z., (1999). Air-Conditioning and Refrigeration, Mechanical Engineering Handbook, CRC Press LLC, pp. 9/34-56.
- YILMAZ, T., (2001), Soğutma Teknolojisi , Çukurova University publish no:37.

CURRICILUM VITAE

Yunus Emre TÜRKOĞLU was born in Adana, 1984. After being graduated from Büyükkoyuncu Science High School, he enrolled in Mechanical Engineering Department of Çukurova University. He continued his Master of Science education in Mechanical Engineering Department of Çukurova University in 2006. He has been working as an engineer in Tosyalı Iron-Steel plant in İskenderun since 2008.

GÜNCEL YAKIT FİYATLARININ KARŞILAŞTIRMA TABLOSU^[1]

(06 Nisan 2009 tarihinde, KDV HARİÇ)

YAKITLAR	YAKIT ALT ISIL DEĞERİ	YAKIT ÜST ISIL DEĞERİ	YAKIT BİRİM FİYATI [1]			ALT ISIL DEĞERE göre 1000 kcal için YAKIT FİYATI [2]			ÜST ISIL DEĞERE göre 1000 kcal için YAKIT FİYATI [3]		
			kr [1]	USD [5]	Avro [5]	kr (3)	USD (5)	Avro (5)	kr (4)	USD (5)	Avro (5)
DOĞALGAZ	kcal/m ³	kcal/m ³	kr/m ³	USD/m ³	Avro/m ³	kr (3)	USD (5)	Avro (5)	kr (4)	USD (5)	Avro (5)
(BOTAŞ) PROSES, BUHAR ve ELEKTRİK KULLANICILARI için. (Kesintisiz) SAMAYİ	8.250	9.155	65.3586	0,4167	0,3081	7.92	0,0505	0,0373	7.14	0,0455	0,0337
(BOTAŞ) PROSES, BUHAR ve ELEKTRİK KULLANICILARI için. (Kesintisiz) OSB	8.250	9.155	65.9956	0,4207	0,3111	8.00	0,0510	0,0377	7.21	0,0460	0,0340
(BOTAŞ) PROSES, BUHAR ve ELEKTRİK KULLANICILARI için. (Kesintisiz) SAMAYİ	8.250	9.155	65.9956	0,4207	0,3111	8.00	0,0510	0,0377	7.21	0,0460	0,0340
(İGDAŞ) Serbest Tüketici Olan PROSES ve BUHAR KULLANICILARI için SAMAYİ	8.250	9.155	68.0430	0,4338	0,3208	8.25	0,0526	0,0389	7.43	0,0474	0,0350
(İGDAŞ) Serbest Tüketici Olmayan PROSES ve BUHAR KULLANICILARI için SAMAYİ	8.250	9.155	78.3930	0,4998	0,3696	9.50	0,0606	0,0448	8.56	0,0546	0,0404
ELEKTRİK	kcal/kWh	kcal/kWh	kr/kWh	USD/kWh	Avro/kWh	kr (3)	USD (5)	Avro (5)	kr (3)	USD (5)	Avro (5)
SAMAYİ Elektrik											
TEK TERİM - Alpak Enerji Tek Zamanlı Tarife - TEDAŞ	860	860	15.1020	0,0963	0,0712	17.56	0,1119	0,0828	17.56	0,1119	0,0828
KOHUT Elektrik											
Tek Zamanlı Tarife - TEDAŞ	860	860	20.9760	0,1337	0,0889	24.39	0,1555	0,1150	24.39	0,1555	0,1150
TİCARETHANE Elektrik											
Tek Zamanlı Tarife - TEDAŞ	860	860	24.5100	0,1563	0,1155	28.50	0,1817	0,1344	28.50	0,1817	0,1344

APPANDIX A2

TOSYALI DEMİR ÇELİK SAN.A.Ş

Organize Sanayi Bölgesi
Sanseki
İSKENDERUN/HATAY

ALARKO

Carrier

ALARKO CARRIER
SANAYİ VE TİCARET A.Ş.

ANKARA BÜROSU
SEDAT SEMAİT SOK. NO:48
06550 ÇANKAYA - ANKARA

Telefon : (0312) 440 79 18 Pbx
Faks : (0312) 440 79 33 - 440 31 70
Tic. Sic. No : 83928 / 29126
İnternet : info@alrko-carrier.com.tr
TARİH : 15.05.2009
İŞARETİMİZ : K-2009- 7143T
DOSYA NO : G21(UO)29

Teklif Mektubudur

İşin Adı
TOSÇELİK PROJESİ (HAVA SOĞUTMALI SOĞUTMA GRUBU)

İlgi
TOSÇELİK PROJESİ (HAVA SOĞUTMALI SOĞUTMA GRUBU) işinize malzeme temini hakkında

Toplu Bedeli
31.900 EUR + KDV
Yalnız otuzbirbindokuzyüz Euro + KDV

Teslim Süresi
Siparişinizi müteakip 8-10 hafta içerisinde

Teslim Şekli
Yurüçi nakliye ve sigorta bedeli tarafınıza ait olmak üzere, şantiyelerizde araç üzerinde

Ödeme Şekli
Toplu bedel+KDV'nin %35'i siparişte peşin ve nakten, %45'i malzeme teslim tarihli, %20'si teslim tarihi+30gün tarihli döviz bazlı çek veya tam pullu senet ile ödenecektir. Ödemelerde ödeme tarihindeki TCMB efektif satış kurları esas alınacaktır.

Garanti
Malzemelerimiz imalat ve malzeme hatalarına karşı fatura tarihinden itibaren iki yıl süreyle garantimiz altındadır.

Opsiyon
Teklifimiz değişen şartlara göre uyarlanacaktır.

Saygılarımızla,
ALARKO

Carrier

ALARKO CARRIER
SANAYİ VE TİCARET A.Ş.

SEDAT SEMAİT SOK. NO:48
06550 ÇANKAYA - ANKARA

Tamer Şenyuva
Sistem Satış Müdürü

Omer Uçuncu
Sistem Satış Müdür Yrd.

ALARKO



Carrier

ALARKO CARRIER
SARAY VE TİCARET A.Ş. ANKARA BÜROSU

Tarih : 15.05.2009
Referans : K-2009- 7143T
Deşya No : G21(UO)29

GÜRBÜZ MAKİNA

No	Malzeme	Miktar	Birim Fiyat	Tutar
1	SOĞUTMA GRUBU CARRIER mamulü, aşağıda belirtilen kapasite ve çalışma şartlarında, hava soğutmalı AQUASNAP soğutma grubu. Gruplar; motor, kompresör, içten soğutma devreli borulara haiz yalıtımlı evaporatör, kondenser, gerekli tüm güvenlik ve çalıştırma cihazlarına kapsayan dış hava korumalı elektronik kontrol merkezinden oluşmuş olup, fabrikada her türlü bonu ve kablo bağlantısı, gaz-yag sağı ve kaçak kontrolü yapılmış olarak tek parça hâlinde ve yerine yerleştirmeye hazır olarak gelirler. GENEL ÖZELLİKLER Tip: 30 RB 232 Soğutma kapasitesi : 221.4 kW Grubun Çektiği Güç: 69,1 kW Bağımsız Gaz Devre Sayısı: 2 Soğutucu Akışkan: R-410 Kompresör Tipi: Scroll Kompresör Sayısı: 4 Kompresör Fanları: Flying Bird-Düşük Ses Seviyeli Evap.Su Giriş/Çıkış Sıcaklığı: 12/7°C Kondenser Tipi: Hava Soğutmalı Dış Hava Sıcaklığı: 37°C	1	31.900,	31.900,
			Toplam Tutar.....(Euro)	31.900
			Genel Toplam.....	31.900



ALARKO CARRIER
SARAY VE TİCARET A.Ş.
SATICI MÜŞTERİ İLİŞKİLERİ BÖLÜMÜ
FİYAT ENERJİ VE KURUMLAR
KURUMU
TEL: 0312 244 10 10

APPANDIX A3

TOSYALI DEMİR ÇELİK SAN.A.Ş
Organize Sanayi Bölgesi
Sarıteki
İSKENDERUNHATAY

ALARKO



ALARKO CARRIER
SANAYİ VE TİCARET A.Ş.

ANKARA BÜROSU
SEDAT SİDAMI SOK. NO:44
06530 ÇANKAYA - ANKARA

Telefon : (0312) 440 77 10 Pbx
Faks : (0312) 440 77 30 - 440 11 70
Tic. Sic. No : 81936 / 29776
İnternet : www.alarko-carrier.com.tr
TARİH : 15.05.2009
İŞARETİMİZ : K-2009- 7147T
DOSYA NO : G21(UO)29

Teklif Mektubudur

İşin Adı
TOSÇELİK PROJESİ (ABSORBSİYONLU SOĞUTMA GRUBU)

İlgi

TOSÇELİK PROJESİ (ABSORBSİYONLU SOĞUTMA GRUBU) işinize malzeme temini hakkında

Toplu Bedeli

84.700 EUR + KDV

Yalnız seksendörtbinyediyüz Euro + KDV

Teslim Süresi

Siparişinizi müteakip 12-14 hafta içerisinde

Teslim Şekli

Yurtiçi nakliye ve sigorta bedeli tarafınıza ait olmak üzere, şantiyelerinde araç üzerinde

Ödeme Şekli

Toplu bedel+KDV'nin %35'i siparişe peşin ve nakten, %45'i malzeme teslim tarihli, %20'si teslim tarihi+30gün tarihli döviz bazlı çek veya tam pullu senet ile ödenecektir. Ödemelerde ödeme tarihindeki TCMB efektif satış kurları esas alınacaktır.

Garanti

Malzemelerimiz imalat ve malzeme hatalarına karşı fatura tarihinden itibaren iki yıl süreyle garantimiz altındadır.

Opsiyon

Teklifimiz değişen şartlara göre uyarlanacaktır.

Saygılarımızla,

ALARKO



ALARKO CARRIER
SANAYİ VE TİCARET A.Ş.

ORGANİZE SANAYİ BÖLGESİ
SARITEKI

İSKENDERUNHATAY

Tamer Şenyuva
Sistem Satış Müdürü

Omer Üçüncü
Sistem Satış Müdür Yrd.



CARRIER CHINA OPERATION
ABSORPTION CHILLER SELECTION DATA SHEET

CUSTOMER	Demo			
DATE	Ocak 8, 2009			
Unit Size	-	16DN015		
Cooling Capacity	kW	235		
Heating Capacity	kW	443		
Chilled Water	Inlet Temp	°C	12,0	
	Outlet Temp	°C	7,0	
	Flow Rate	m ³ /hr	40	
	Pressure Drop	kPa	88,9	
	Fluid Type	-	Water	
	Fouling Factor	m ² -K/kW	0,08500	
	Pass Number	-	5	
	Pipe Connection Size	mm	65	
Cooling Water	Inlet Temp	°C	30,0	
	Outlet Temp	°C	35,0	
	Flow Rate	m ³ /hr	69	
	Pressure Drop	kPa	24,1	
	Fluid Type	-	Water	
	Fouling Factor	m ² -K/kW	0,08500	
	Pass Number	A	-	2
		C	-	1
	Pipe Connection Size	mm	100	
	Hot Water	Inlet Temp	°C	50,8
Outlet Temp		°C	60,0	
Flow Rate		m ³ /hr	40	
Pressure Drop		kPa	78,4	
Fluid Type		-	Water	
Fouling Factor		m ² -K/kW	0,08500	
Pass Number		-	5	
Pipe Connection Size		mm	65	
Nature Gas (LNG)	Heating Value(LHV)	kcal/Nm ³	11000,00	
	Consumption (Cooling)	Nm ³ /hr	14	
	Consumption (Heating)	Nm ³ /hr	37	
Exhaust Gas	Outlet Connection Size	mm	280×210	
Electrical	Power Supply	-	380V-3Ph-50Hz	
	Power	Solution Pump	kW	3,70
		Refrigerant Pump	kW	0,40
		Burner	kW	0,75
		Capacity	KVA	10,8
Charge	LBr Solution (55wt%)	kg	880	
	Refrigerant (R20)	kg	400	
	Alcohol	L	4,0	
Dimension	Length	mm	3531	
	Width	mm	1866	
	Height	mm	2058	
Weight	Rigging	kg	5060	
	Operating	kg	6780	
Max. Working Pressure	CHW Side	MPa	1,0	
	CW Side	MPa	1,0	
Water Pipe Connection	-	GB Flange		
Applied Code	-	Maker Standard		
Shipping Method	-	1 piece		
Painting Color	-	Carrier Green Gray		
Thermal Insulation	-	Job Site		
Burner Specification	Burner Company	-	Maker Standard	
	Burner Type	-	Gas Burner	

ALARKO

Carrier

ALARKO CARRIER
SANAYİ VE TİCARET A.Ş. ANKARA BÜROSU

Tarih : 15.05.2009
Referans : K-2009- 7147T
Dosya No : G21(UO)/29
TOSYALI DEMİR ÇELİK SAN.A.Ş

No	Malzeme	Miktar	Birim Fiyat	Tutar
1	ABSORBSİYONLU CHILLER SOĞUTMA GRUBU CARRIER'İN mamülü absorpsiyonlu doğalgaz ısıtmalı su soğutma gruplarıdır. Ekli örnekte seçim çıktısı verilmiştir. GENEL ÖZELLİKLER Tip: 16DN015 Soğutma kapasitesi : 235 kW Isıtma kapasitesi:443 kW Soğutma tarafı: Su rejimi:30/35 C Basınç Düşümü:24.1 kPa Isıtma tarafı: Su rejimi:50/60 C Basınç Düşümü 76.4 kPa Doğalgaz Isıtma Kapasitesi:11000 kcal/Nm ³	1	84.700,	84.700,
			Toplam Tutar.....(Euro)	84.700
			Genel Toplam.....	84.700

ALARKO
ALARKO CARRIER
SANAYİ VE TİCARET A.Ş.
ANKARA BÜROSU
TOSYALI DEMİR ÇELİK SAN.A.Ş.